www.oncotarget.com Oncotarget, 2020, Vol. 11, (No. 28), pp: 2718-2739

Research Paper

Genetic analysis of the cooperative tumorigenic effects of targeted deletions of tumor suppressors *Rb1*, *Trp53*, *Men1*, and *Pten* in neuroendocrine tumors in mice

Eugenia Y. Xu[1,2,3], Evan Vosburgh[4,5], Chung Wong[1,7], Laura H. Tang[6] and Daniel A. Notterman[3]

[1]Rutgers Cancer Institute of New Jersey, Rutgers, The State University of New Jersey, New Brunswick, NJ 08903, USA

[2]Department of Pediatrics, Robert Wood Johnson Medical School, Rutgers, The State University of New Jersey, New Brunswick, NJ 08901, USA

[3]Department of Molecular Biology, Princeton University, Princeton, NJ 08544, USA

[4]Department of Medicine, Veterans Administration Hospital, West Haven, CT 06516, USA

[5]Department of Medicine, Yale University School of Medicine, New Haven, CT 06510, USA

[6]Department of Pathology, Memorial Sloan-Kettering Cancer Center, New York, NY 10065, USA

[7]Current address: Regeneron Inc., Tarrytown, NY 10591, USA

Correspondence to: *Eugenia Y. Xu,* ***email***: *exu@princeton.edu*
Daniel A. Notterman, ***email***: *dan1@princeton.edu*

Keywords: neuroendocrine tumors; *RB1; Trp53; PTEN; Men1*

Received: *April 20, 2020* ***Accepted***: *June 15, 2020* ***Published***: *July 14, 2020*

ABSTRACT

Genetic alterations of tumor suppressor genes (TSGs) are frequently observed to have cumulative or cooperative tumorigenic effects. We examined whether the TSGs *Rb1*, *Trp53*, *Pten* and *Men1* have cooperative effects in suppressing neuroendocrine tumors (NETs) in mice. We generated pairwise homozygous deletions of these four genes in insulin II gene expressing cells using the Cre-LoxP system. By monitoring growth and examining the histopathology of the pituitary (Pit) and pancreas (Pan) in these mice, we demonstrated that pRB had the strongest cooperative function with PTEN in suppressing PitNETs and had strong cooperative function with Menin and TRP53, respectively, in suppressing PitNETs and PanNETs. TRP53 had weak cooperative function with PTEN in suppressing pituitary lesions. We also found that deletion of *Pten* singly led to prolactinomas in female mice, and deletion of *Rb1* alone led to islet hyperplasia in pancreas. Collectively, our data indicated that pRB and PTEN pathways play significant roles in suppressing PitNETs, while the Menin-mediated pathway plays a significant role in suppressing PanNETs. Understanding the molecular mechanisms of these genes and pathways on NETs will help us understand the molecular mechanisms of neuroendocrine tumorigenesis and develop effective preclinical murine models for NET therapeutics to improve clinical outcomes in humans.

INTRODUCTION

Human pituitary neuroendocrine tumors (PitNETs) are the third most common intracranial neoplasms and represent approximately 10–25% of all primary intracranial tumors [1, 2]. Pituitary carcinomas are highly aggressive and represent < 1% of pituitary tumors. The pituitary gland sits at the pituitary fossa and contains anterior, intermediate and posterior lobes. The anterior lobe mainly secretes prolactin, growth hormone (GH), adrenocorticotropin (ACTH), thyroid-stimulating hormone (TSH), and gonadotropin [follicle-stimulating hormone (FSH) and luteinizing hormone (LH)]. The posterior lobe is considered an extension of the hypothalamus and secretes oxytocin and anti-diuretic hormone (ADH). The intermediate lobe is located between anterior and posterior lobes. It secretes melanocyte-stimulating hormone (MSH) during fetal life but is small or absent in adults. Although PitNETs are

generally benign monoclonal neoplasms, they can cause significant morbidity including visual disturbances caused by mass effects that lead to compression of adjacent structures, and/or deregulated hormone secretion, and then mortality [3, 4]. PitNETs can be characterized based on cell of origin and the types of hormone secreted, like prolactinomas (40–57%), nonfunctioning (15–37%), and ACTH-secreting (1.6–5.9%) [5–7]. Pituitary pathogenesis is challenging to study due to its unique biology and behavior. The molecular mechanism of tumor progression in the pituitary remains unclear.

Human pancreatic neuroendocrine neoplasms are classified as either well-differentiated (WD) pancreatic neuroendocrine tumors (PanNETs) or islet cell tumors and poorly differentiated (PD) pancreatic neuroendocrine carcinomas (PanNECs) [8, 9]. Based on Ki67 proliferation rate, WD-PanNETs are also classified as grade 1 (G1), grade 2 (G2), and grade 3 (G3) PanNETs with Ki67 index of < 3%, 3–20% and > 20%, respectively [9, 10]. PD-PanNECs are not derived from pancreatic islet cells; they are inevitably high grade with Ki67 index of > 20%. PanNETs are the second-most common pancreatic malignancy but only represent 1–2% of pancreatic tumors, and are far less aggressive than the most common pancreatic ductal adenocarcinoma. Even though less aggressive, PanNETs have limited treatment options if not resectable at diagnosis [11]. WD-PanNETs and PD-PanNECs develop as a result of different genetic alterations [12]. Understanding the molecular mechanism of tumorigenesis may aid in the development of novel therapeutic options.

Tumorigenesis is a multistep process involving alterations of oncogenes and/or tumor suppressor genes (TSGs) in a single cell. In contrast to oncogene activation, tumors resulting from TSG inactivation usually require both alleles to be lost, according to the Knudson's "two-hit" hypothesis [13]. *TP53* and retinoblastoma susceptibility gene (*RB1*) encode classic tumor suppressors and are commonly inactivated or deregulated in human cancers [14–16]. Genetic mutations of *TP53* are observed in about 4% of PanNETs and the mutation rate for *RB1* appears to be very low. While the rates are low, mutations in both genes are often associated with aggressive PD-PanNECs [10]. Genetic mutations of *RB1* and *TP53* in human PitNETs are even less common [17–24]. Two studies have indicated that approximately 90% of PitNETs have at least one RB pathway gene silenced due to promoter methylation [25, 26]. Additionally, in rare cases *RB1* has been found with epigenetic mutations in the promoter region in PitNETs [27, 28] suggesting that inactivation of the RB pathway contributes to the development of PitNETs. *Rb1* mouse models develop highly penetrant pituitary tumors—ACTH-secreting tumors in most cases [29, 30], evidence that supports RB pathway playing a role in pituitary tumorigenesis. In mice, deletion of the *Trp53* gene leads to a wide spectrum of tumors but does not lead to NETs. However, deletion of *Trp53* accelerates NET development in $Rb1^{+/-}$ mice suggesting that TRP53 plays a role in NE tumorigenesis [31, 32]. Therefore, although *RB1* and *TP53* may not mutate frequently, both the TP53 and RB pathways are compromised in human NETs.

Menin is a 68 KDa protein encoded by the *MEN1* gene, a tumor suppressor gene mutated in Multiple Endocrine Neoplasia Type 1 (MEN1) [33]. MEN1 is an autosomal dominant tumor syndrome with high penetrance characterized by the presence of several endocrine tumors derived from pituitary, parathyroid, and pancreatic islet cells [34]. *MEN1* mutations are also observed in around 44% of non-familial human PanNETs, most often WD G1/G2 PanNETs [35, 36]. Several *Men1* mouse models generated by targeted mutation of the *Men1* gene [37–39] effectively mimic the tumor spectrum in humans. The PTEN (Phosphatase and TENsin homolog) tumor suppressor, a key negative regulator of the PI3K/AKT pathway encoding a lipid phosphatase, is located on a genomic region that frequently suffers loss of heterozygosity (LOH) in different types of advanced human cancers. Genetic mutations of *PTEN* are observed in about 7–26.4% of human PanNETs [35, 36, 40–45]. Reduced PTEN expression and increased PI3K/AKT pathway activity have been observed in human patients with pituitary tumors [46, 47]. Compound mice with concomitant deletions of *Men1* and *Pten* develop PitNETs and PanNETs and mice with $p18^{-/-}$ $Pten^{+/-}$ mutations develop PitNETs [48, 49], suggesting that PTEN plays a role in pituitary and pancreatic islet tumorigenesis. But whether deletion of *Pten* alone induces PitNETs in mice is still unknown.

Tissue-specific homozygous deletion of TSGs in mice provides a powerful tool to understand the genetic basis of tumor progression. Functional cooperation between loss-of-function mutations targeting TSGs is commonly required for the progression of a normal cell into a cancerous one. We have investigated how pairwise deletions of TSGs cooperate in neuroendocrine tumorigenesis in mice. Double heterozygous *Men1* and *Rb1* knockout mice have been reported to develop the same tumor spectrum as the respective single knockout mice [50, 51]. The absence of cumulative effects from *Men1* and *Rb1* mutations leads to the suggestion that Menin and pRB are in the same molecular pathway of tumor suppression. However, *Men1* deletion mice develop *pars distalis* prolactinomas and *Rb1* deletion mice develop *pars intermedia* tumors of pituitary, suggesting that the functions of Menin and pRB may not fully overlap. Here we investigate the question of whether *Men1* and *Rb1* have cooperative tumorigenic effects on NETs using tissue-specific double homozygous deletions of *Men1* and *Rb1* in mice. To systematically test how deficiencies in the TSGs *Rb1*, *Men1*, *Trp53*, and *Pten* cooperate in tumorigenesis in mice, we have conditionally inactivated these genes in pairs in insulin II-expressing cells using the Cre-LoxP system in which Cre recombinase is under the control of

Rat Insulin II gene Promoter (RIP-Cre). We used a targeted system as mouse models bearing complete *Rb1*, *Men1*, and *Pten* gene loss display embryonic lethality. We report here the characterization of PitNETs and PanNETs with double homozygous deletions of TSGs (Table 1) and illustrate that pRB has the strongest cooperative function with PTEN in suppressing PitNETs and has strong cooperative function with Menin and TRP53, respectively, in suppressing PitNETs and PanNETs in mice. Our data demonstrate that the pRB and PTEN pathways play significant roles in suppressing PitNETs while the Menin pathway plays a significant role in suppressing PanNETs in mice.

RESULTS

Rb1 and *Men1* function cooperatively to accelerate PitNETs and death

To investigate whether Menin and pRB function cooperatively in neuroendocrine tumorigenesis, we generated compound $Men1^{flox/flox}$ $Rb1^{flox/flox}$ RIP-Cre (MRbR) mice with concomitant homozygous deletions of *Men1* and *Rb1* in the pancreas and pituitary through a series of crosses (Figure 1A). Mice with other genetic combinations generated from these series of crosses were examined as well. The genotypes of the compound mice were confirmed by PCR analysis using genomic tail DNA (Figure 1B). We monitored the survival of a cohort of double homozygous deletions MRbR mice, alongside control mice—wild-type control $Men1^{flox/flox}$ $Rb1^{flox/flox}$ (MRb) without RIP-Cre transgene, the single homozygous deletion $Men1^{flox/flox}$ RIP-Cre (MR) and $Rb1^{flox/flox}$ RIP-Cre (RbR) (Figure 1C). Wild-type control MRb and single deletion MR mice were viable during the study period of thirty-four weeks, as previously reported for MR mice [37]; Single deletion RbR mice started dying at sixteen weeks, had a median survival of twenty-one weeks and did not live beyond thirty-one weeks; double homozygous deletions MRbR mice started dying at ten weeks, had a median survival of thirteen weeks and did not live beyond twenty-one weeks. These data indicated that concomitant loss of *Rb1* and *Men1* accelerated death ($p < 0.0001$) more than a single deletion; and *Rb1* deletion alone had a more severe effect on survival than *Men1* deletion alone ($p < 0.0001$).

To understand the cause of death of these mice, the sick mice were autopsied. PitNETs were observed in both MRbR, and RbR mice (Figure 1E). The nineteen sick MRbR mice (9F/10M) and the twenty-three sick RbR mice (8F/15M) all showed symptoms such as loss of vision, tilted head/body—symptoms consistent with those described in human patients with PitNETs and as reported in $Men1^{flox/flox}$ $Pten^{flox/flox}$ RIP-Cre (MPR) mice [48]. Wild-type control MRb and single deletion MR mice of the same age displayed normal or slightly enlarged pituitaries, respectively. Evaluation of the pituitary size in a cohort of MRbR, RbR, MR, and MRb mice as they age displayed that pituitaries grew fastest in MRbR mice (Figure 1D). RbR mice grew dramatically faster and bigger pituitaries than MR and wild-type control MRb mice. Death of MRbR and RbR mice was due to PitNETs. Western blot analysis confirmed that Menin and/or RB1 expression was knocked down in the pituitary in representative MRbR, MR, and RbR mice (data not shown). Concomitant loss of *Rb1* and *Men1* in mice resulted in an earlier onset of PitNETs compared to single deletion of *Men1* and *Rb1*, suggesting that pRB and Menin function cooperatively to suppress pituitary tumorigenesis. Earlier onset of PitNETs and death in RbR mice than MR mice suggested that pRB plays a more significant role in suppressing pituitary tumorigenesis compared to Menin.

To understand the pituitary origin of these tumors, the PitNETs from MRbR ($n = 11$) and RbR ($n = 8$) mice and the pituitaries from wild-type control MRb ($n = 11$) mice were immunohistochemically stained for prolactin, GH, and ACTH. MRb mice showed staining consistent with a normal pituitary–heterogeneous staining of prolactin, GH, and ACTH in the anterior lobe; negative staining of prolactin and GH in the intermediate and posterior lobes; positive ACTH staining in the intermediate lobe but negative staining in the posterior lobe, which is as reported, ACTH-secreting corticotrophs represent the major cell type in the pars intermedia in mice [52]. PitNETs from MRbR and RbR mice showed negative staining of prolactin and GH, but positive staining of ACTH (Figure 2A). Serum ELISA assays confirmed the ACTH-secreting PitNETs (Figure 2B, prolactin and GH results not shown). RbR mice showed variable levels of serum ACTH concentration because RbR mice developed PitNETs at a wider age range than MRbR mice. These PitNETs arose from the intermediate lobe, as reported in *Rb1* mutation mice [53]. Consistent with ACTH-secreting PitNETs, MRbR ($p = 0.6612$), and RbR ($p = 0.7535$) mice did not show gender bias in death and pituitary size as mice aged (Figure 2C and 2D). The PitNETs developed in MRbR mice were attributable to the loss of pRb, supporting that pRB plays a significant role in suppressing pituitary tumorigenesis compared to Menin.

Rb1 and *Men1* function cooperatively to accelerate PanNETs

We next investigated the effect of the concomitant loss of *Rb1* and *Men1* in the pancreas in comparison with the effect of single *Men1* or *Rb1* deletion. We evaluated the pancreas of double deletions MRbR ($n = 36$) and single deletion RbR ($n = 46$) mice along with wild-type control MRb ($n = 62$) and single deletion MR ($n = 78$) mice macroscopically and evaluated the histopathology of the pancreas in a subset of the mice. Wild-type control MRb mice showed normal pancreas both macroscopically and microscopically with few small, round islets with normal distribution of α cells (Figure 3A and 3B). Macroscopic

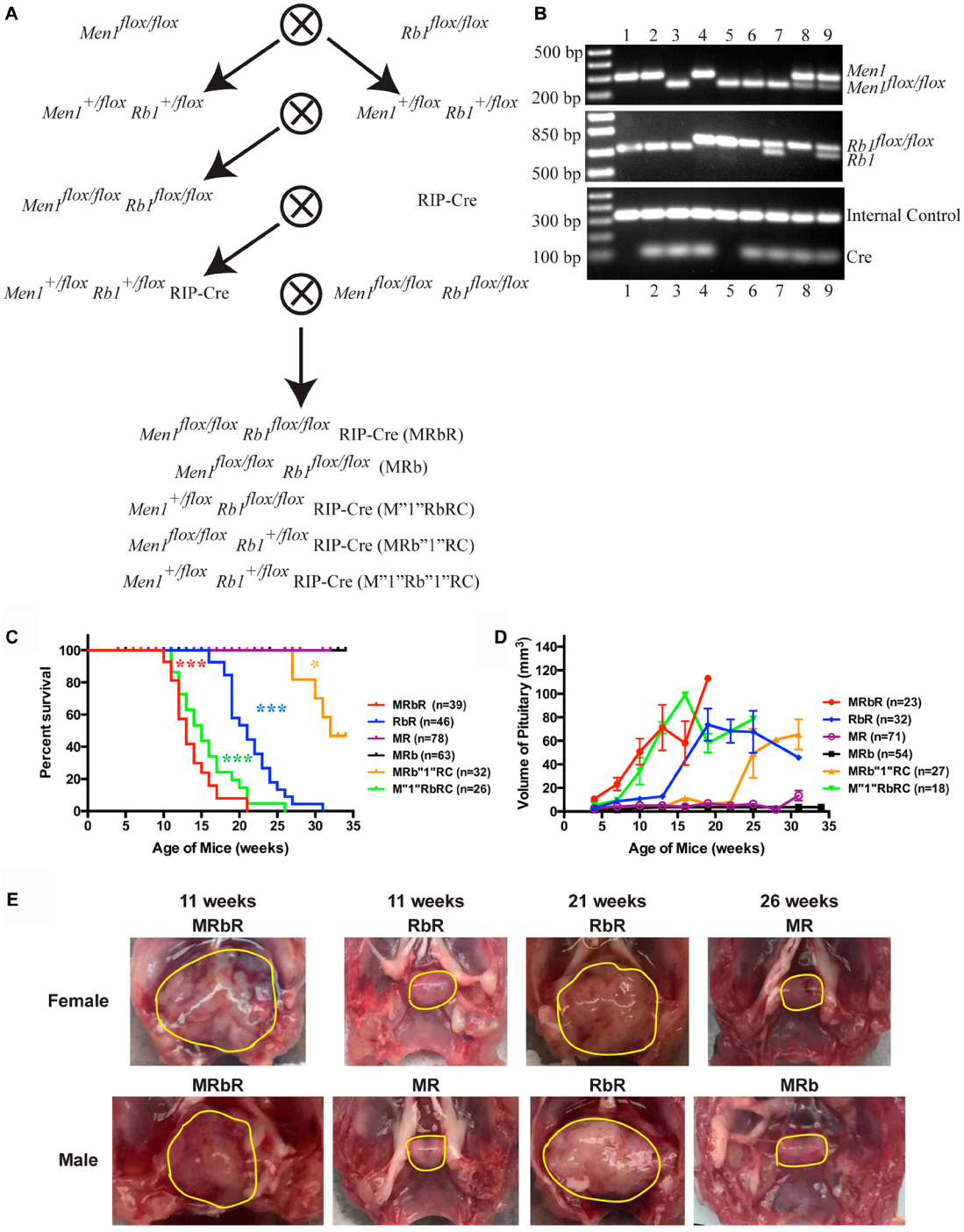

Figure 1: Concomitant loss of *Men1* and *Rb1* decreased survival and accelerated PitNET development in MRbR mice. (**A**) Diagram of the strategy used to generate compound mice MRbR and littermates MRb, M"1"RbRC, MRb"1"RC, and M"1"Rb"1"RC. (**B**) Representative genotyping results of the litters in A by PCR analysis using tail genomic DNA. Genotypes of each lane: 1-WT, 2-RIP-Cre, 3-$Men1^{flox/flox}$ RIP-Cre (MR), 4-$Rb1^{flox/flox}$ RIP-Cre (RbR), 5-$Men1^{flox/flox}$ $Rb1^{flox/flox}$ (MRb), 6-$Men1^{flox/flox}$ $Rb1^{flox/flox}$ RIP-Cre (MRbR), 7-$Men1^{flox/flox}$ $Rb1^{+/flox}$ RIP-Cre (MRb"1"RC), 8-$Men1^{+/flox}$ $Rb1^{flox/flox}$ RIP-Cre (M"1"RbRC), and 9-$Men1^{+/flox}$ $Rb1^{+/flox}$ RIP-Cre (M"1"Rb"1"RC). (**C**) Kaplan–Meier survival curves showed significantly shorter life spans ($p < 0.0001$) in double deletions MRbR mice than single deletion MR, RbR, and corresponding wild-type control MRb mice; The survival curve of MRbR mice had no significant difference from that of M"1"RbRC mice. M"1"RbRC mice showed significantly shorter life spans than RbR mice ($p < 0.0001$), and MRb"1"RC mice ($p < 0.0001$). MRb"1"RC mice showed shorter life spans than MR mice ($p < 0.0176$). (**D**) Evaluation of the sizes of pituitaries in three-week intervals starting at 4 weeks in double deletions MRbR mice and their littermates, single deletion MR and RbR mice at scheduled autopsy showed that the pace of pituitary growth is consistent with the pattern of the survival curves in C. (**E**) Gross pathology of pituitary shown from representative MRbR, RbR, MR, and MRb female and male mice at specified age. Normal pituitary is cylindrical in shape as seen in wild-type control MRb mice. Pituitaries or PitNETs were circled in yellow lines inside the mouse skull. $^{***}p$-value < 0.0001; $^{*}p$-value < 0.05.

examination of pancreas in RbR mice showed normal and abnormal pancreas. In evaluating the histology of pancreas sections from RbR mice (n = 42), only one RbR mouse pancreas at eighteen weeks (n = 20 mice between age 18–31 weeks) showed tumor and the rest only showed hyperplasia (Figure 3B and 3C). Almost all RbR mice developed hyperplasia without pancreatic tumors in pancreas but all sick RbR mice developed PitNETs in brain, supporting that death of RbR mice was due to development of PitNETs (Table 2). MR mice showed PanNETs after twenty-three weeks and with increasing penetrance as mice aged (data not shown [37]), indicating that deletion of *Rb1* had less effect on islet tumorigenesis than deletion of *Men1*.

Macroscopic examination of pancreas in double deletion MRbR mice demonstrated multifocal nodules after ten weeks in some mice (Figure 3A). Evaluation of the histology of pancreas sections in MRbR (n = 35) mice indicated that pancreatic tumors developed as early as eight to nine weeks and reached around 50% of mice by ten weeks (Figure 3B and 3C), much earlier than in mice with a single deletion of *Men1* or *Rb1*. MRbR mice

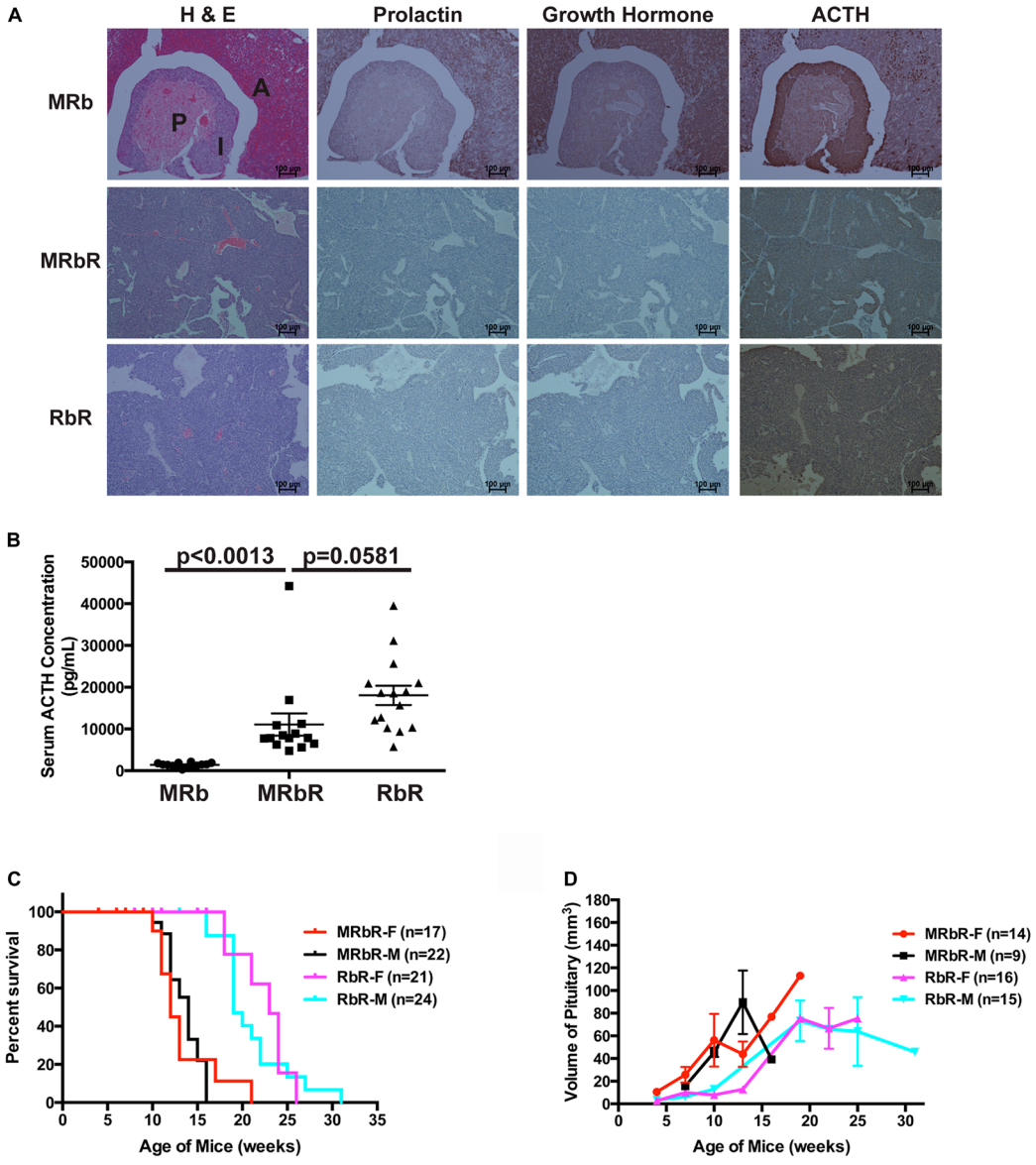

Figure 2: MRbR mice developed ACTH-secreting PitNETs. (**A**) H & E, IHC staining for prolactin, growth hormone, and ACTH on pituitary sections in MRb, MRbR, and RbR mice. Anterior lobe (A), Intermediate lobe (I), and Posterior lobe (P) of normal pituitary in MRb mice are shown in the H & E section. (**B**) Serum ACTH levels using ELISA assays in MRb, MRbR, and RbR mice confirmed that the PitNETs from MRbR and RbR mice were ACTH-secreting tumors. Serum ACTH levels between MRbR and RbR mice were not significantly different (p = 0.0581), but were significantly higher than that in MRb mice of the same age and sex as that of MRbR mice (p < 0.0013). (**C** and **D**) No gender bias was observed in MRbR and RbR mice for survival or pituitary growth as they age. (C) Survival curve. The survival curves of MRbR (p = 0.6612) and RbR (p = 0.7535) mice showed no statistical significances between female and male mice. (D) Pituitary growth.

Table 1: Summary of the phenotypes of mice with various genotypes

Acronyms	Genotypes	Onset of Death*	Types of PitNETs**	Histology of pancreas/Onset of PanNETs**
MRbR	*Men1*$^{flox/flox}$ *Rb1*$^{flox/flox}$ RIP-Cre	10 weeks	ACTH-secreting PitNETs	Hyperplasia to WD G1/G2 PanNETs/10 weeks
MRb	*Men1*$^{flox/flox}$ *Rb1*$^{flox/flox}$	None	NA	Normal /NA
MR	*Men1*$^{flox/flox}$ RIP-Cre	None	Prolactinomas	Hyperplasia to WD G1/G2 PanNETs/23 weeks
RbR	*Rb1*$^{flox/flox}$ RIP-Cre	16 weeks	ACTH-secreting PitNETs	Hyperplasia/NA
M"1"RbRC	*Men1*$^{flox/+}$ *Rb1*$^{flox/flox}$ RIP-Cre	11 weeks	ACTH-secreting PitNETs	Hyperplasia/NA
MRb"1"RC	*Men1*$^{flox/flox}$ *Rb1*$^{flox/+}$ RIP-Cre	27 weeks	Prolactinomas	Hyperplasia to PanNETs/NA
M"1"Rb"1"RC	*Men1*$^{flox/+}$ *Rb1*$^{flox/+}$ RIP-Cre	None	NA	Normal/NA
PR	*Pten*$^{flox/flox}$ RIP-Cre	None	Prolactinomas	Hyperplasia/NA
P	*Pten*$^{flox/flox}$	None	NA	Normal/NA
M"1"PRC	*Men1*$^{flox/+}$ *Pten*$^{flox/flox}$ RIP-Cre	15 weeks	Prolactinomas	Hyperplasia/NA
MP"1"RC	*Men1*$^{flox/flox}$ *Pten*$^{flox/+}$ RIP-Cre	23 weeks	Prolactinomas	Hyperplasia to PanNETs/NA
M"1"P"1"RC	*Men1*$^{flox/+}$ *Pten*$^{flox/+}$ RIP-Cre	None	NA	Normal/NA
PRbR	*Pten*$^{flox/flox}$ *Rb1*$^{flox/flox}$ RIP-Cre	4 weeks	ACTH-secreting PitNETs	Normal/NA
PRb	*Pten*$^{flox/flox}$ *Rb1*$^{flox/flox}$	None	NA	Normal/NA
53PR	*Trp53*$^{flox/flox}$ *Pten*$^{flox/flox}$ RIP-Cre	17 weeks	Enlarged pituitary	Hyperplasia/NA
53P	*Trp53*$^{flox/flox}$ *Pten*$^{flox/flox}$	None	NA	Normal/NA
53RbR	*Trp53*$^{flox/flox}$ *Rb1*$^{flox/flox}$ RIP-Cre	9 weeks	ACTH-secreting PitNETs	Hyperplasia to G3 PanNETs/9 weeks
53Rb	*Trp53*$^{flox/flox}$ *Rb1*$^{flox/flox}$	None	NA	Normal/NA

Notes: *None, no death during the study period; **NA, not available.

with pancreatic tumors may not be sick but all sick mice developed PitNETs, supporting that death of MRbR mice was due to development of PitNETs (Table 3). The ratio of islets area per pancreas area in mice from fifteen to seventeen weeks was significantly greater for MRbR mice ($p < 0.0001$) compared to single deletion MR mice who had significantly more islets area per pancreas area than single deletion RbR mice ($p < 0.0003$) who had significantly more islets area per pancreas area than wild-type control MRb mice (Figure 3D). Collectively, concomitant deletion of *Men1* and *Rb1* accelerated tumor development in pancreas. Menin plays a more significant role in suppressing islet tumorigenesis than pRB.

MRbR pancreatic tumors displayed immunoreactivity to insulin, and the neuroendocrine markers chromogranin A (data not shown) and synaptophysin, indicating that these tumors were PanNETs (Figure 3B). The Ki-67 index of MRbR tumors was 2.8% ($n = 5$), specifying these were WD G1/G2 PanNETs. MRbR mice displayed lower blood glucose levels and higher serum insulin levels compared to control MRb mice of the same age (Figure 3E and 3F), indicating these PanNETs were insulinomas.

Rb1 plays a more significant role than Men1 in suppressing PitNETs

We compared pituitary tumorigenesis in mice with concomitant heterozygous deletion of *Men1* and homozygous deletion of *Rb1* (M"1"RbRC), concomitant homozygous deletion of *Men1* and heterozygous deletion of *Rb1* (MRb"1"RC), concomitant heterozygous deletion of *Men1* and heterozygous deletion of *Rb1* (M"1"Rb"1"RC). Survival, pathology and histology of these mice up to thirty-five weeks demonstrated: double heterozygous M"1"Rb"1"RC mice were viable and healthy during the study period and M"1"RbRC mice showed significantly shorter life spans than MRb"1"RC mice ($p < 0.0001$) (Figure 1C). The median survival of M"1"RbRC mice was fifteen weeks and that of MRb"1"RC mice was thirty-two weeks. M"1"RbRC mice had significantly shorter life spans than single deletion RbR mice ($p < 0.0001$) and MRb"1"RC mice had significantly shorter life spans than single deletion MR mice ($p < 0.0176$), indicating that suppression of death by pRB and Menin was dosage-dependent.

Autopsies of the sick mice displayed large PitNETs in all brains, and normal or abnormal pancreas, indicating that M"1"RbRC and MRb"1"RC mice were sick due to development of PitNETs (Figure 4A). The sizes of PitNETs at death were not significantly different between M"1"RbRC and MRb"1"RC mice ($p = 0.1885$), as well as not significantly different from MRbR mice ($p = 0.8032$ and $p = 0.3614$) respectively. Wild-type control MRb mice of the same age and sex as MRbR mice showed normal pituitary. The survival curve between M"1"RbRC and MRbR mice had no significant difference ($p = 0.1325$) (Figure 1C). However, the survival curve between MRbR mice and MRb"1"RC mice was significantly different ($p < 0.0001$). The growth pace of the pituitaries as mice aged was consistent with the pattern of their survival curves, suggesting that faster growth of PitNETs of these mice

led to shorter life spans (Figure 1D) and indicating that deletion of *Men1* had less effect on pituitary tumorigenesis than deletion of *Rb1*.

Consistent with RbR mice developing ACTH-secreting PitNETs and MR mice developing prolactinomas, M"1"RbRC mice (n = 8) developed ACTH-secreting PitNETs and MRb"1"RC mice (n = 8) developed prolactinomas (Figure 4C). Further, female MRb"1"RC mice showed significantly shorter life spans ($p < 0.0016$) than male MRb"1"RC mice while female

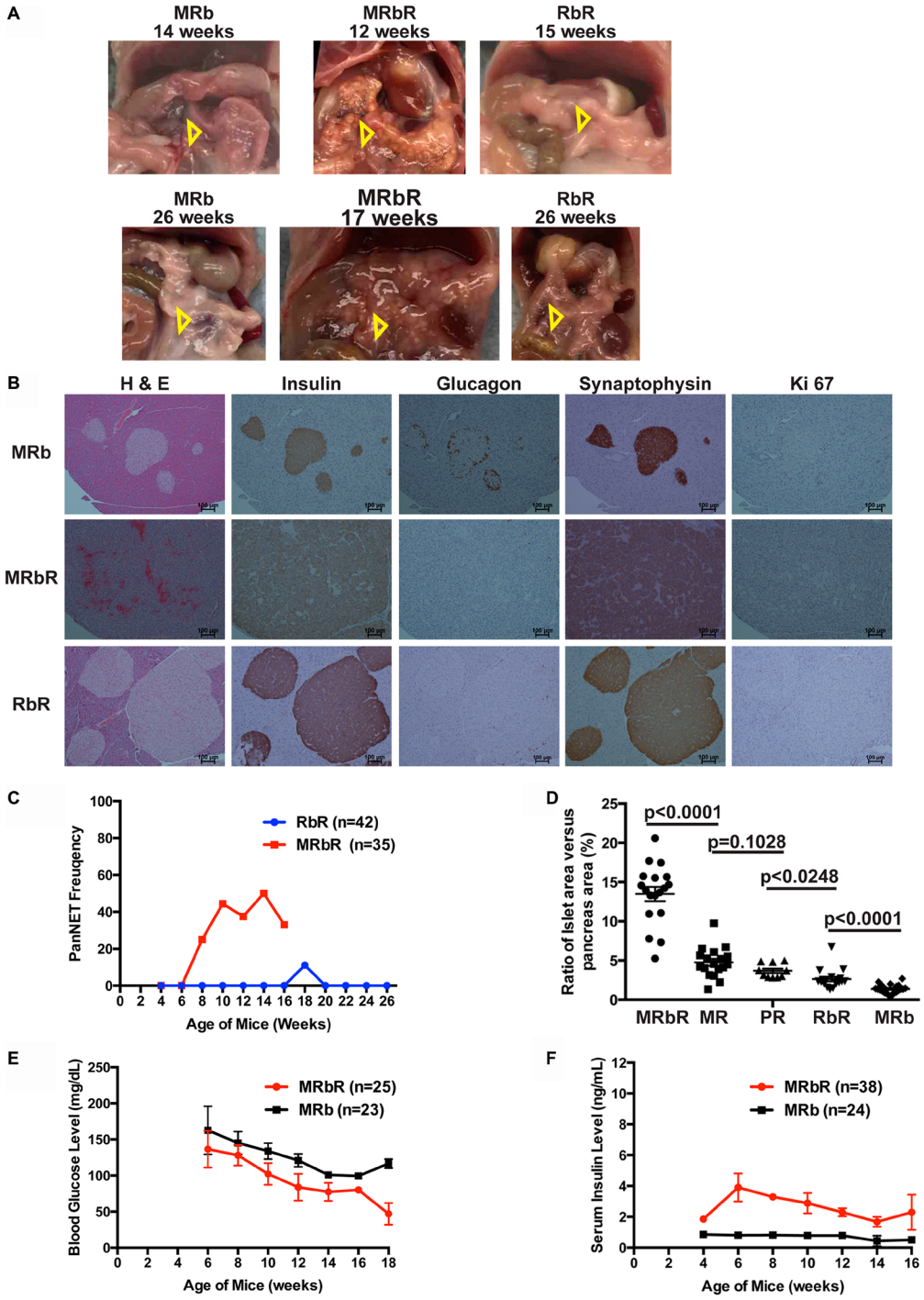

Figure 3: Concomitant loss of *Men1* and *Rb1* accelerated PanNET development in MRbR mice. (**A**) Gross pathology of pancreas in MRb, MRbR and RbR mice at the specified age. Pancreas was shown with open triangle inside the mouse abdomen. (**B**) H & E, IHC staining of Insulin, Glucagon, Synaptophysin and Ki-67 of MRb, MRbR and RbR pancreas sections. (**C**) Frequency of PanNETs in MRbR and RbR mice at scheduled autopsy. (**D**) Quantitative comparison of the ratio of the islets area per pancreas area from double deletions MRbR, single deletion MR, PR, and RbR, and wild-type control MRb mice of 15–17 weeks with shown p-values. (**E**) Blood glucose level in MRbR and MRb mice as they age (**F**) Serum insulin level in MRbR and MRb mice as they age.

Table 2: Histology of pancreas, size of pituitary and health condition in RbR mice

Age of Mice (weeks)	Mouse Number	Histology of Pancreatic islets	Size of pituitary (L × W × H mm)*	Mouse health condition
4	RbR mouse 1	Normal/ hyperplasia	3 × 1 × 1	Healthy
4	RbR mouse 2	Normal/ hyperplasia	3 × 1 × 1	Healthy
4	RbR mouse 3	Normal/ hyperplasia	3 × 1 × 1	Healthy
6	RbR mouse 4	Normal/ hyperplasia	4 × 2 × 1.5	Healthy
6	RbR mouse 5	Normal/ hyperplasia	3 × 1.5 × 1.5	Healthy
6	RbR mouse 6	Normal/ hyperplasia	3 × 2 × 2	Healthy
8	RbR mouse 7	Normal/ hyperplasia	4 × 2.5 × 2	Healthy
8	RbR mouse 8	Hyperplasia	3 × 2 × 2	Healthy
10	RbR mouse 9	Hyperplasia	3 × 2 × 2	Healthy
10	RbR mouse 10	Normal/ hyperplasia	4 × 2 × 2	Healthy
10	RbR mouse 11	Hyperplasia	4 × 2 × 2	Healthy
10	RbR mouse 12	Hyperplasia	4 × 2 × 2	Healthy
10	RbR mouse 13	Hyperplasia	5 × 4 × 2	Healthy
10	RbR mouse 14	Hyperplasia	4.5 × 3.5 × 2	Healthy
10	RbR mouse 15	Hyperplasia	3 × 2 × 2	Healthy
10	RbR mouse 16	Hyperplasia	4 × 3.5 ×2	Healthy
10	RbR mouse 17	Hyperplasia	3 × 2 × 2	Healthy
12	RbR mouse 18	Hyperplasia	NA	Healthy
14	RbR mouse 19	Normal/ hyperplasia	3.5 × 3.5 × 2	Healthy
16	RbR mouse 20	Normal/ hyperplasia	NA	Healthy
16	RbR mouse 21	Normal/ hyperplasia	NA	Healthy
16	RbR mouse 22	Normal/ hyperplasia	NA	Sick
18	RbR mouse 23	Hyperplasia	NA	Healthy
18	RbR mouse 24	Hyperplasia	NA	Healthy
18	RbR mouse 25	Tumor	NA	Sick
18	RbR mouse 26	Hyperplasia	NA	Sick
18	RbR mouse 27	Hyperplasia	7.5 × 5 × 2.5	Sick
18	RbR mouse 28	Hyperplasia	8 × 5 × 2.5	Sick
18	RbR mouse 29	Hyperplasia	NA	Sick
18	RbR mouse 30	Normal/ hyperplasia	NA	Sick
18	RbR mouse 31	Hyperplasia	NA	Sick
20	RbR mouse 32	Hyperplasia	7 × 6 × 3	Sick
20	RbR mouse 33	Hyperplasia	10 × 8 × 3	Sick
20	RbR mouse 34	Hyperplasia	8 × 6 × 3	Sick
22	RbR mouse 35	Hyperplasia	7 × 6 × 3	Sick
22	RbR mouse 36	Normal/ hyperplasia	8 × 6 × 3	Sick
22	RbR mouse 37	Hyperplasia	5 × 5 × 3	Sick
24	RbR mouse 38	Hyperplasia	10 × 6 × 3	Sick
24	RbR mouse 39	Hyperplasia	8 × 7.5 × 3	Sick
26	RbR mouse 40	Hyperplasia	8 × 6 × 3	Sick
27	RbR mouse 41	Hyperplasia	8 × 4 × 2	Sick
31	RbR mouse 42	Hyperplasia	7 × 5 × 2.5	Sick

Note: *NA, not available (i.e., the size of pituitary was not measured).

M"1"RbRC had similar life spans (p = 0.5267) to male M"1"RbRC mice, confirming a gender bias in mice developing prolactinomas (Figure 4B). Collectively, the suppression of PitNETs by pRB and Menin was dosage-dependent and pRB plays a more significant role in suppressing PitNETs over Menin.

Table 3: Histology of pancreas, size of pituitary and health condition in MRbR mice

Age of Mice (weeks)	Mouse Number	Histology of Pancreatic islets	Size of pituitary (L × W × H mm)	Mouse health condition
4	MRbR mouse 1	Hyperplasia	3.5 × 2 × 1.5	Healthy
6	MRbR mouse 2	Hyperplasia	5 × 3 × 1.5	Healthy
6	MRbR mouse 3	Hyperplasia	NA	Healthy
6	MRbR mouse 4	Hyperplasia	4 × 3.5 × 2	Healthy
6	MRbR mouse 5	Hyperplasia	NA	Healthy
6	MRbR mouse 6	Hyperplasia	5 × 3 × 1.5	Healthy
6	MRbR mouse 7	Hyperplasia	4 × 3 × 2.5	Healthy
8	MRbR mouse 8	Hyperplasia	5 × 5 × 2.5	Healthy
8	MRbR mouse 9	Hyperplasia	5 × 5 × 2.5	Healthy
8	MRbR mouse 10	Hyperplasia	NA	Healthy
8	MRbR mouse 11	Tumor	NA	Healthy
10	MRbR mouse 12	Hyperplasia	5 × 5 × 2.5	Healthy
10	MRbR mouse 13	Hyperplasia	NA	Sick
10	MRbR mouse 14	Tumor	NA	Healthy
10	MRbR mouse 15	Tumor	NA	Healthy
10	MRbR mouse 16	Tumor	NA	Healthy
10	MRbR mouse 17	Hyperplasia	6 × 6 × 2.5	Healthy
10	MRbR mouse 18	Hyperplasia	6 × 5 × 2.5	Healthy
10	MRbR mouse 19	Hyperplasia	10 × 8 × 3	Sick
10	MRbR mouse 20	Tumor	5 × 5 × 3	Sick
12	MRbR mouse 21	Hyperplasia	NA	Healthy
12	MRbR mouse 22	Hyperplasia	6 × 5 × 3	Sick
12	MRbR mouse 23	Tumor	NA	Sick
12	MRbR mouse 24	Hyperplasia	5 × 5 × 3	Sick
12	MRbR mouse 25	Hyperplasia	5 × 3.5 × 3	Sick
12	MRbR mouse 26	Tumor	NA	Sick
12	MRbR mouse 27	Hyperplasia	NA	Healthy
12	MRbR mouse 28	Tumor	5 × 5 × 3	Sick
14	MRbR mouse 29	Tumor	10 × 7.5 × 3	Sick
14	MRbR mouse 30	Tumor	7 × 5 × 3	Sick
14	MRbR mouse 31	Hyperplasia	8 × 4 × 2	Sick
14	MRbR mouse 32	Hyperplasia	5 × 5 × 2.5	Healthy
16	MRbR mouse 33	Hyperplasia	5 × 5 × 3	Sick
16	MRbR mouse 34	Hyperplasia	7 × 7 × 3	Sick
16	MRbR mouse 35	Tumor	12 × 6 × 3	Sick

Note: *NA, not available (i.e., the size of pituitary was not measured).

Pten deletion alone led to PitNETs

Since it has been reported that PTEN may play a role in suppressing PitNETs in mice [48, 49], we evaluated whether the deletion of *Pten* alone led to PitNETs. We constructed $Pten^{flox/flox}$ RIP-Cre (PR) mice and monitored the growth of mice along with control $Pten^{flox/flox}$ (P) mice for up to forty-three weeks. All mice were viable and healthy. Autopsies of the brains of these mice every other week starting at seven weeks showed that pituitaries grew gradually in PR mice and eventually developed into tumors in female mice while a normal size pituitary was maintained in both female and male control P mice (Figure 5A and 5B). Gender bias was observed in pituitary growth and tumor development. Female mice displayed faster growth of pituitaries and developed earlier PitNETs. Consistent with this observation, significantly elevated serum prolactin levels were observed in female PR mice as PitNETs developed (Figure 5C), while serum GH levels were normal in both PR and P mice (data not shown) and serum ACTH levels were slightly increased in both male and female PR mice older than twenty-seven weeks compared to age- and sex-matched control P mice (Figure 5D). Female PR mice with PitNETs had dramatically

elevated prolactin levels, normal GH levels, and slightly but significantly increased ACTH levels compared to age matched control female P mice (Figure 5E–5G), further confirmed by IHC staining (data not shown). These results indicated that PitNETs in female PR mice originated from anterior lobe while intermediate lobe was slightly enlarged as the pituitary grew in both female and male PR mice. The PitNETs were prolactinomas. Taken together, deletion of *Pten* alone led to PitNETs in mice, and PTEN plays a role in anterior and intermediate lobes of pituitary.

Pten plays a more significant role than Men1 in suppressing PitNETs

Since PR mice developed PitNETs earlier and faster than MR mice (Figures 1D and 5B), we investigated whether *Pten* plays a more important role in pituitary tumorigenesis than *Men1* using the same strategy as above for *Rb1*. We performed survival, pathological and histological analyses of mice with these genotypes: $Men1^{flox/+}$ $Pten^{flox/flox}$ RIP-Cre (M"1"PRC), $Men1^{flox/flox}$ $Pten^{flox/+}$ RIP-Cre (MP"1"RC) and $Men1^{flox/+}$ $Pten^{flox/+}$ RIP-Cre (M"1"P"1"RC) up to thirty-four weeks. These mice were the littermates of MPR mice described in [48]. Double heterozygous M"1"P"1"RC mice were viable and healthy during the study period. The Kaplan–Meier survival curve demonstrated that M"1"PRC mice had shorter life spans than MP"1"RC mice ($p < 0.0039$) (Figure 6A). The median survival of M"1"PRC mice was twenty-six weeks and that of MP"1"RC mice was twenty-nine weeks during the study period. MP"1"RC mice ($p < 0.0353$) and M"1"PRC mice ($p < 0.0001$) had decreased

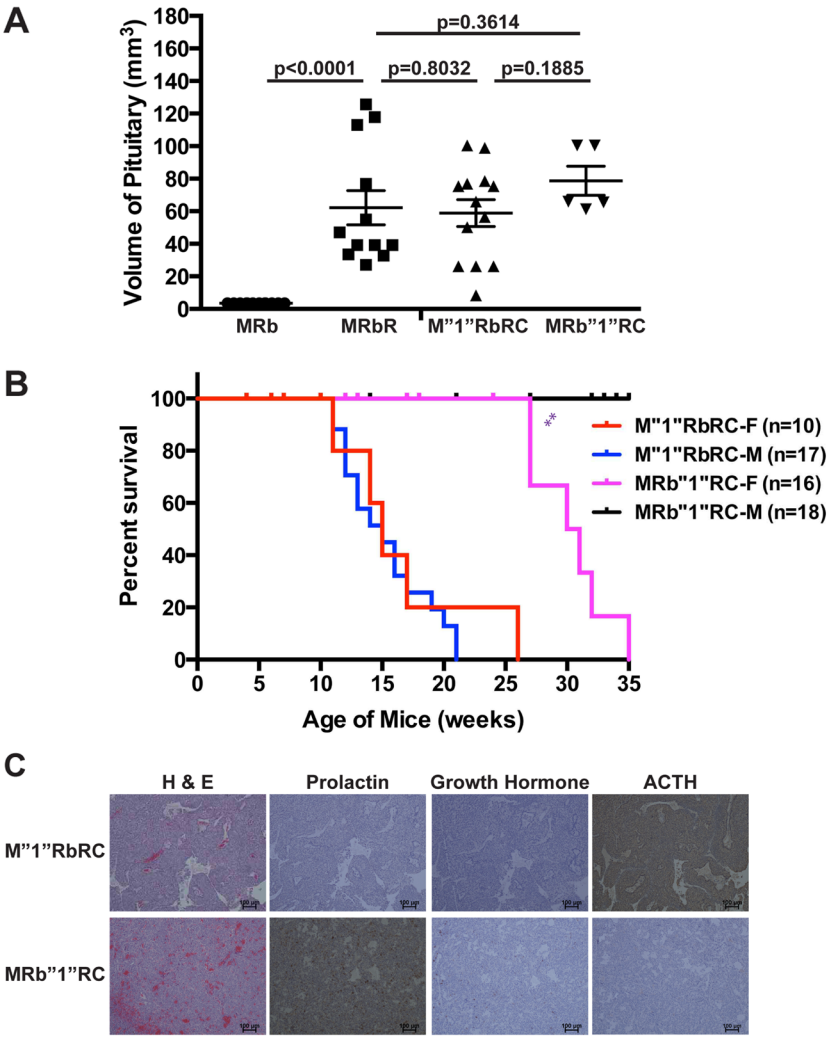

Figure 4: TSG *Rb1* plays a more significant role in suppressing PitNETs compared to *Men1*. (**A**) The sizes of PitNETs in MRbR, M"1"RbRC and MRb"1"RC at death were not significantly different from each other as shown *p*-values. Wild-type control mice MRb that were sex and age matched to double deletions MRbR mice showed normal pituitary. (**B**) Gender bias in survival was observed in MRb"1"RC mice ($p < 0.0016$) but was not observed in M"1"RbRC mice ($p = 0.5267$). (**C**) H & E, IHC staining of prolactin, growth hormone, and ACTH showed that M"1"RbRC mice developed ACTH-secreting PitNETs, while MRb"1"RC mice developed prolactinomas. $^{**}p$-value < 0.01.

survival compared to MR and PR mice, respectively, but longer life spans than MPR mice ($p < 0.0001$). Evaluation of the growth pace of the pituitaries in the cohort of mice in two-week intervals was consistent with the pattern of the survival curve suggesting that faster development and larger PitNETs resulted in shorter life spans (Figure 6B), indicating these mice were sick due to development of PitNETs. Besides this, pituitaries grew faster in MPR mice than M"1"PRC and MP"1"RC mice; faster in M"1"PRC mice than PR mice and faster in MP"1"RC mice than MR mice (Figures 6B, 5B, and 1D), indicating that the suppression of PitNETs by PTEN and Menin was dosage-dependent and deletion of *Pten* had a stronger effect on pituitary tumorigenesis than deletion of *Men1*.

Consistent with MR and PR mice developing prolactinomas, both M"1"PRC ($n = 10$) and MP"1"RC ($n = 10$) mice developed prolactinomas (Figure 6C) based on IHC staining of prolactin, GH, and ACTH. Consistent with prolactinomas development in these mice, a gender bias in survival was observed (Figure 6D). Female M"1"PRC ($p < 0.0305$) and MP"1"RC ($p < 0.0025$) mice had significantly shorter life spans than corresponding male

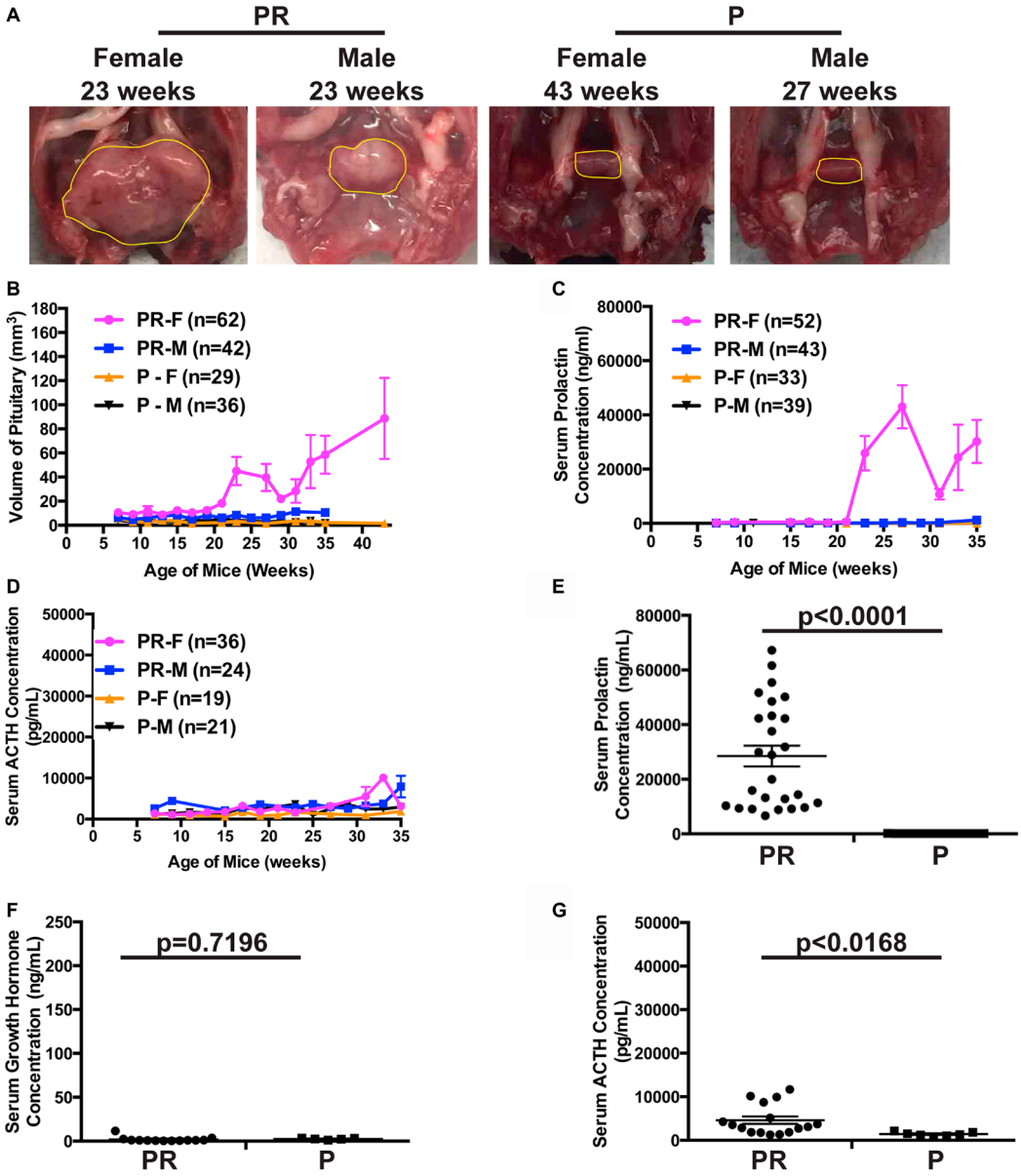

Figure 5: Deletion of TSG *Pten* alone led to PitNETs. (**A**) Gross pathology of pituitary in female and male PR and control P mice. Normal pituitary is cylindrical in shape as seen in control P mice. Pituitaries and PitNETs were circled in yellow lines inside the mouse skull. (**B**) Evaluation of the sizes of pituitaries in three-week interval starting at 6 weeks in female and male PR and control P mice at scheduled autopsy. (**C**) Serum prolactin levels measured by ELISA assay in female and male PR and control P mice as they age. (**D**) Serum ACTH levels measured by ELISA assay in female and male PR and P mice as they age. (**E–G**). Serum ELISA hormone assays in female PR mice with PitNETs and control female P mice of the same age with shown *p*-values. (E) prolactin, (F) growth hormone, and (G) ACTH.

mice. Collectively, PTEN plays a more important role in suppressing PitNETs than Menin.

Rb1 and *Pten* function cooperatively to accelerate PitNETs and death

If both PTEN and pRB play important roles in suppressing PitNETs, we predicted that mice with double deletion of *Pten* and *Rb1* would exhibit cumulative effects on pituitary tumorigenesis. We constructed tissue-specific double homozygous deletions of *Pten* and *Rb1* in pancreas and pituitary using the same strategy as used for MRbR mice (Figure 7A), confirmed the correct genotypes of the compound mice by PCR analysis using tail DNA (Figure 7B), and monitored the growth of these double homozygous deletions $Pten^{flox/flox}$ $Rb1^{flox/flox}$ RIP-Cre (PRbR) and wild-type control $Pten^{flox/flox}$ $Rb1^{flox/flox}$ (PRb) mice. Consistent with our discovery of more important roles for *Rb1* and *Pten* than *Men1* in pituitary, PRbR ($n = 14$) mice showed symptoms of PitNETs such as loss of vision, tilted head/body, and circular gait path starting at four weeks and did not live beyond ten weeks (Figure 7C), indicating that PitNETs developed much earlier in PRbR mice than in single deletion RbR and PR mice and double deletions

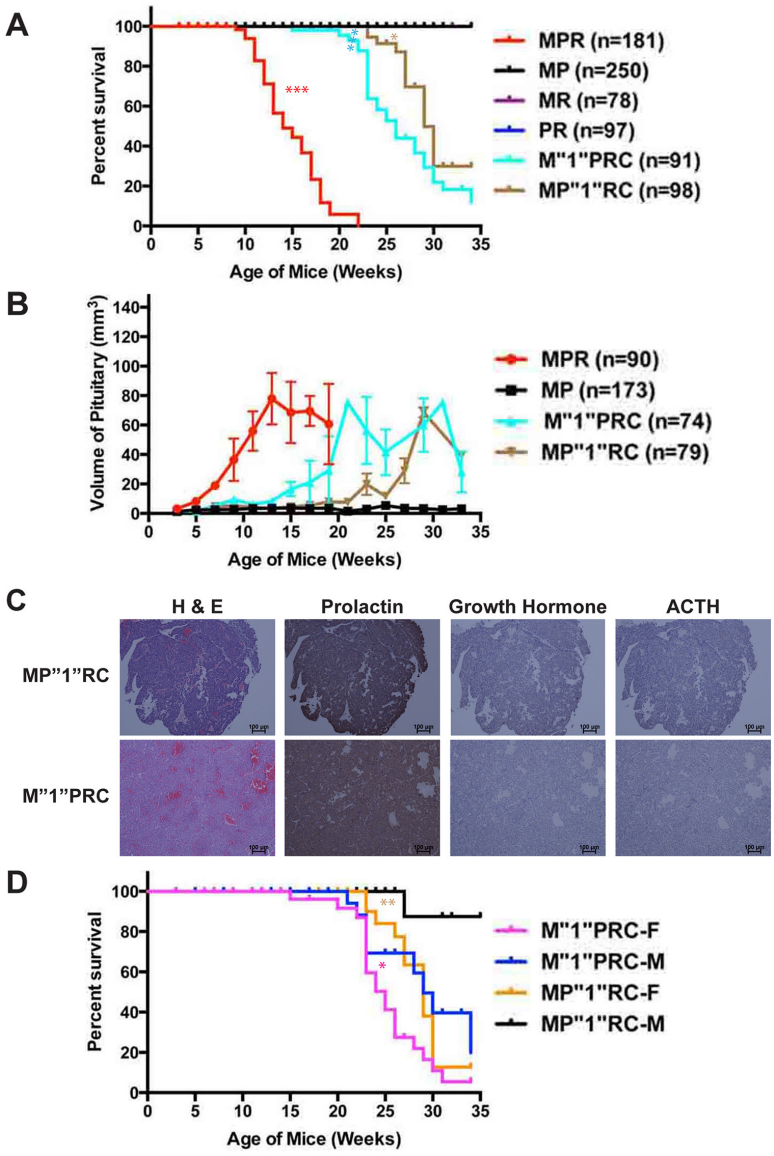

Figure 6: *Pten* plays a more significant role in suppressing PitNETs compared to *Men1*. (**A**) Survival curve of M"1"PRC and MP"1"RC mice in comparison with MPR, MR, PR, and MP mice. M"1"PRC mice showed significantly longer life span than MPR mice ($p < 0.0001$), but shorter life span than MP"1"RC mice ($p < 0.0039$) and PR mice ($p < 0.0001$). MP"1"RC mice showed shorter lifer span than MR mice ($p < 0.035$). (**B**) Evaluation of the pituitary sizes of M"1"PRC and MP"1"RC mice in comparison with MPR and MP mice as they age. (**C**) H & E, and IHC staining of prolactin, growth hormone and ACTH showed that both M"1"PRC and MP"1"RC mice developed prolactinomas. (**D**) Gender bias in survival was observed in M"1"PRC and MP"1"RC mice. Female M"1"PRC ($p < 0.0305$) and MP"1"RC ($p < 0.0025$) mice showed shorter life sans than corresponding male mice. $^{***}p < 0.0001$, $^{**}p < 0.01$, $^{*}p < 0.05$.

MRbR and MPR mice [48]. Wild-type control PRb mice and single deletion PR and RbR mice were viable and healthy up to twelve weeks.

Autopsies of the brains showed that PRbR mice had large PitNETs, with sizes at death that were almost the same as the PitNETs of MRbR and MPR at death (Figures 7D, 7E, 4A, and reference 48). Pancreas in these sick mice was normal macroscopically and histologically. Single deletion PR and RbR mice of the same age only had slightly enlarged pituitaries not significantly different from each other, but both significantly larger than wild-type control PRb mice (Figure 7D and 7E). Serum ELISA hormone assays indicated that PRbR mice had significantly higher serum ACTH concentrations than PRb mice, while serum prolactin and GH concentrations showed no significant difference from PRb mice (Figure 7F–7H). IHC staining of the PitNETs from sick PRbR (n = 8) mice confirmed ELISA assay results (data not shown). Thus, these pituitary tumors in PRbR mice were ACTH-secreting PitNETs. Collectively, our data indicated that deletion of *Rb1* had a cooperative tumorigenesis phenotype with the deletion of *Pten* in pituitary. Both pRB and PTEN play important roles in suppressing PitNETs.

Trp53 and *Pten* had weak cooperative function in suppressing pituitary growth

It has been reported that heterozygous *Rb1* deletion and homozygous *Trp53* deletion has cooperative effects on neuroendocrine tumorigenesis while heterozygous *Men1* deletion and homozygous *Trp53* deletion has non-synergistic effects on tumorigenesis in mice [31, 54]. We asked the question whether *Trp53* has cooperative effects with *Pten* in suppressing NETs. We constructed tissue-specific double homozygous deletions of *Trp53* and *Pten* in pancreas and pituitary (Supplementary Figure 1A) to investigate whether *Trp53* and *Pten* have a cooperative role in NETs. The genotypes of the compound mice were confirmed by PCR analysis using tail genomic DNA (Supplementary Figure 1B). We also constructed double homozygous deletions of *Trp53* with *Rb1* and *Men1*, respectively. Confirmation of the representative genotypes was shown in Supplementary Figure 1C and 1D.

We monitored the growth of compound mice with double deletions $Trp53^{flox/flox}$ $Pten^{flox/flox}$ RIP-Cre (53PR) and wild-type control $Trp53^{flox/flox}$ $Pten^{flox/flox}$ (53P) without RIP-Cre transgene, as well as compound mice with double deletions $Trp53^{flox/flox}$ $Rb1^{flox/flox}$ RIP-Cre (53RbR) and $Trp53^{flox/flox}$ $Men1^{flox/flox}$ RIP-Cre (53MR), single deletion $Trp53^{flox/flox}$ RIP-Cre (53R), and corresponding wild-type controls $Trp53^{flox/flox}$ $Rb1^{flox/flox}$ (53Rb), $Trp53^{flox/flox}$ $Men1^{flox/flox}$ (53M) without RIP-Cre transgene. 53PR mice showed paralysis of hind limbs starting at around seventeen weeks but did not show symptoms of PitNETs. The end point of 53PR mice in this study was the paralysis of hind limbs according to IACUC while control 53P mice of the same age and sex were viable and healthy (Figure 8A). Autopsies of the brains showed that the sick 53PR mice had intact cylindrical, but slightly and significantly enlarged pituitaries (Figure 8B). Histology of the pituitaries showed normal pituitary staining with enlarged intermediate lobe. Serum ELISA hormone assays confirmed the slightly but significantly increased ACTH levels in 53PR mice compared to control 53P mice while prolactin and GH levels were similar (Figure 8C–8E), implying that the intermediate lobe of the pituitaries grew slightly bigger in 53PR mice than control 53P mice.

Similar to what has been reported on mice with homozygous *Trp53* and heterozygous *Men1* or *Rb1* [31, 54], double deletions 53MR mice were viable and healthy up to thirty-two weeks. Double deletions 53RbR mice showed symptoms of PitNETs such as loss of vision, tilted head/body, circular gait path starting at nine weeks and did not live beyond twelve weeks, while wild-type control mice 53Rb, and single deletion mice 53R and RbR of the same age and sex were viable and healthy (Figures 8A and 1C). Large PitNETs were observed in sick 53RbR mice while normal or slightly enlarged pituitaries were found in wild-type control 53Rb or single deletion RbR and 53R mice of the same age (Supplementary Figure 2A). Pituitaries from single deletion 53R mice were similar to those from wild-type control 53Rb mice of the same age, consistent with what has been reported that deletion of *Trp53* did not lead to PitNETs in mice. IHC staining of the PitNETs from 53RbR mice displayed two types of cells: ACTH-secreting tumors (Supplementary Figure 2B, middle panel) and transformed cells with heterogeneous prolactin, GH and ACTH staining (Supplementary Figure 2B, bottom panel). Serum ELISA assays confirmed significantly high ACTH levels in 53RbR mice (data not shown). Thus, pRB has cooperative function with TRP53 in suppressing PitNETs, consistent with the reported cooperative function between the two TSGs [31] and pRB plays a more important role in pituitary tumorigenesis than TRP53.

Since the sizes of the pituitaries at the study endpoint (17–25 weeks) in 53PR mice were slightly but significantly larger than that in single deletion PR and 53R mice or wild-type control 53P mice of the same age but much smaller than that in PRbR, 53RbR and MPR mice at death at younger ages (Figures 8B, 7D, Supplementary Figure 2A, and reference 48), TRP53 and PTEN had weak cooperative function in suppressing pituitary growth in mice.

Further examination of pancreas in the sick 53PR mice showed normal pancreas with increased numbers of small round islets and normal hormone distribution (Figure 8F). Quantitative analysis of the ratio of the islets area per pancreas area indicated that double deletions 53PR mice have significantly increased islets area ratio compared to that in the single deletion 53R and wild-type control 53P mice (Figure 8G), but have no significant difference compared to that in the single deletion PR mice

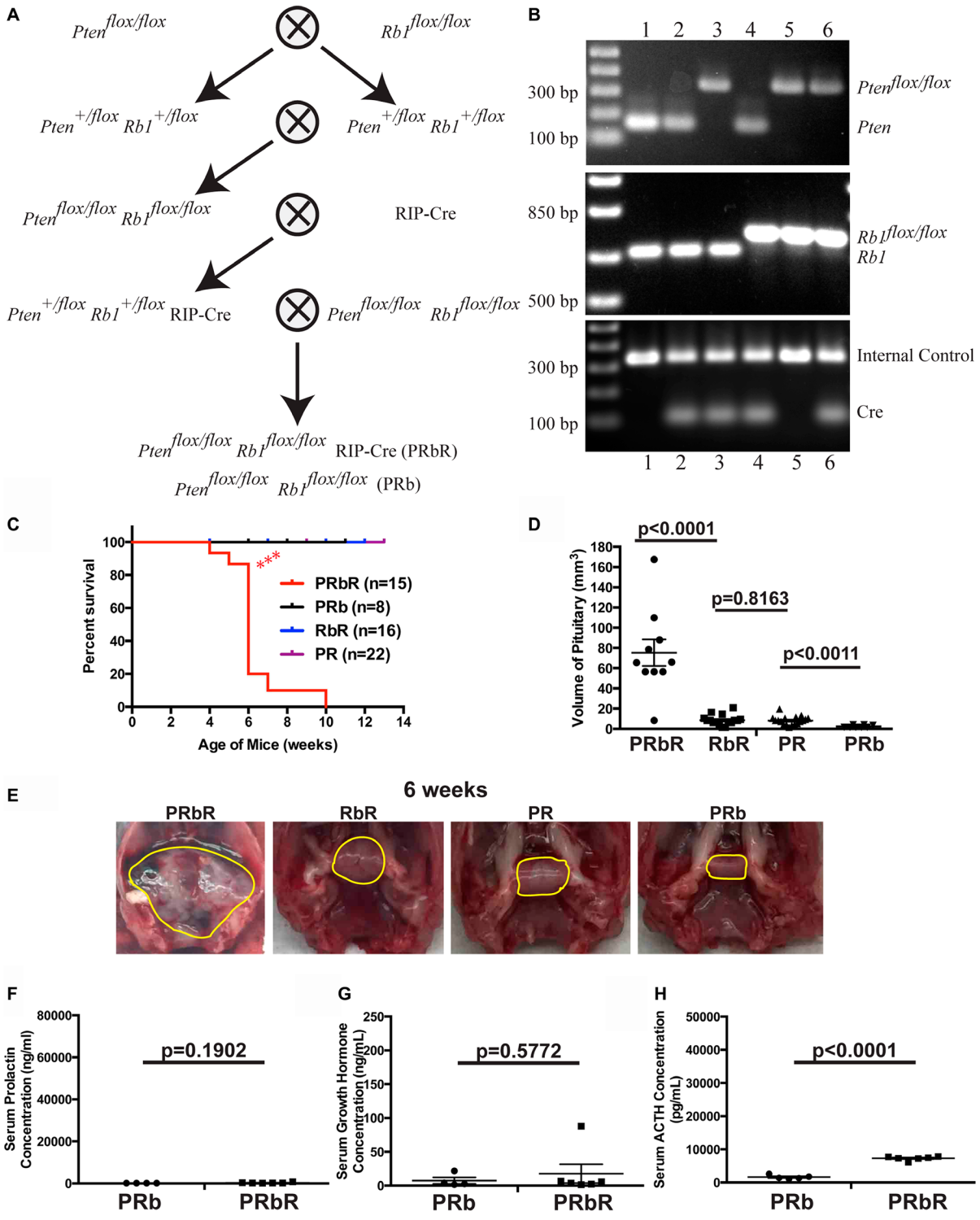

Figure 7: *Pten* and *Rb1* function cooperatively to suppress PitNETs. (**A**) Diagram of the strategy used to generate compound PRbR and PRb mice. (**B**) Representative genotyping results of the litters in A by PCR analysis using tail genomic DNA. Genotypes of each lane: 1-WT, 2-RIP-Cre, 3-$Pten^{flox/flox}$ RIP-Cre (PR), 4-$Rb1^{flox/flox}$ RIP-Cre (RbR), 5-$Pten^{flox/flox}$ $Rb1^{flox/flox}$ (PRb), 6-$Pten^{flox/flox}$ $Rb1^{flox/flox}$ RIP-Cre (PRbR). (**C**) Survival curves showed that concomitant loss of *Rb1* and *Pten* accelerated death in PRbR mice. PRbR mice showed significantly shorter lifer span ($p < 0.0001$) than PR, RbR, and PRb mice. (**D**) The sizes of PitNETs in double deletions PRbR mice at death were significantly larger than that in single deletion RbR, PR, and wild-type control PRb mice of the same age as shown *p*-values. (**E**) Gross pathology of pituitary in double deletions PRbR, single deletion RbR and PR, and wild-type control PRb mice at 6 weeks. A normal pituitary is cylindrical in shape as seen in wild-type control PRb mice. Pituitaries or PitNETs were circled in yellow lines inside the mouse skull. (**F**–**H**) Serum ELISA hormone assays in PRbR and PRb mice with shown *p*-values. (F) prolactin, (G) growth hormone, and (H) ACTH.

(p = 0.9689) (Figure 3D), indicating that the increased numbers of islets in double deletions 53PR mice were due to the effect from deletion of *Pten* alone. Thus, TRP53 and PTEN have no cooperative function in islet lesions at the study end point.

Examination of pancreas in 53MR mice did not show any synthetic islet lesions compared to MR mice alone, which is consistent with what has been reported [54]. Macroscopic examination of the pancreas in 53RbR mice displayed multifocal bloody tumors starting at nine

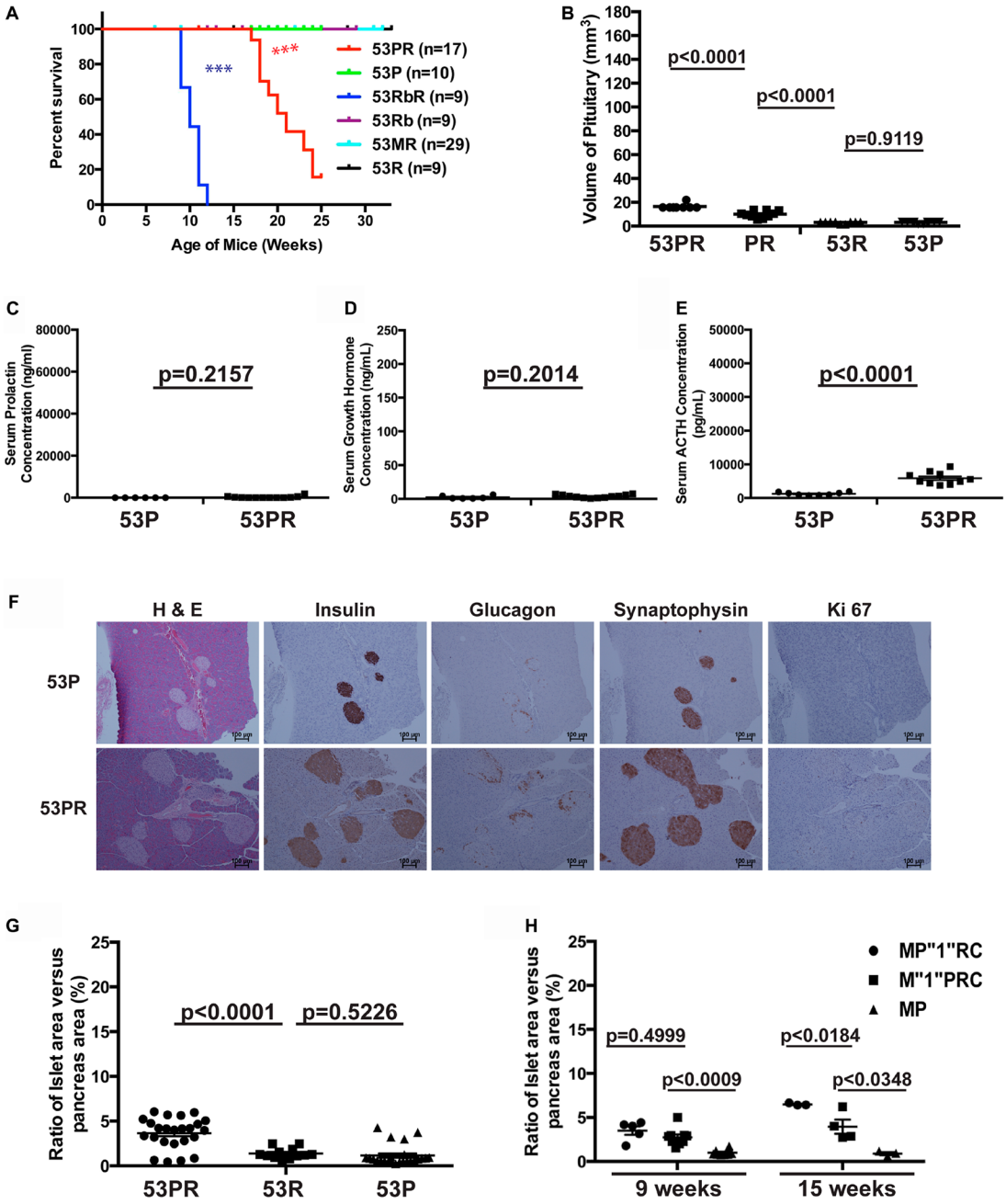

Figure 8: *Trp53* and *Pten* had weak cooperative function in suppressing pituitary growth. (**A**) Survival curve of 53PR and control 53P mice, as well as 53RbR, 53MR and their corresponding control mice. The end point for 53PR mice was the paralysis of hind limbs in our study. 53RbR mice had significantly shorter life spans ($p < 0.0001$) than 53 PR mice, which has significantly shorter life spans ($p < 0.0001$) than 53 MR and wild-type control mice. (**B**) The sizes of pituitaries in 53PR mice at the study endpoint were larger than that in single deletion PR and 53R mice and wild-type control 53P mice matched by age and sex as shown p-values. (**C**–**E**) Serum ELISA hormone assays in 53PR and 53P mice with shown p-values. (C) prolactin (D) growth hormone (E) ACTH. (**F**) H & E, IHC staining of Insulin, Glucagon, Synaptophysin, and Ki67 of pancreas sections from 53P and 53PR mice. (**G**) Quantitative comparison of the ratio of the islets area per pancreas area between 53PR, 53R and 53P mice at 17 weeks with shown p-values. (**H**) Quantitative comparison of the ratio of the islets area per pancreas area among M"1"PRC, MP"1"RC, and wild-type control MP mice at 9 and 15 weeks with shown p-values. $^{***}p < 0.0001$.

weeks. IHC staining of pancreas displayed large tumors with abnormal hormone distribution of α cells - negative staining of glucagon while wild-type control 53Rb mice showed small and round islets with normal peripheral α cell distribution and single deletion 53R (data not shown) and RbR mice of the same age displayed normal and hyperplastic islets (Supplementary Figures 2C and 3B). Immunoreactivity for insulin, neuroendocrine markers chromogranin A and synaptophysin (data not shown) indicated these were PanNETs. Different from WD G1/G2 PanNETs developed in MRbR mice, 53RbR mice developed G3 PanNETs with average Ki67 index of 29.7% (n = 4). Taken together, our data showed that TRP53 did not function cooperatively with PTEN in islet lesions while TRP53 function cooperatively with pRB to suppress PanNETs and had no cooperative function with MEN1 in islet lesions as reported [31, 54]. Thus, TRP53 is dispensable with the intact pRB, but it seems that the role of TRP53 is indispensible in suppressing PitNETs and PanNETs in the absence of pRB.

The paralysis of limbs in 53PR mice may be due to the leaky expression of RIP-Cre transgene in nerves or muscles, which led to double deletions of *Pten* and *Trp53*. We observed paralysis of hind limbs in MPR mice that lived longer than seventeen weeks. We did not observe the paralysis in single deletion mice PR, MR or 53R up to forty-three weeks or longer. The paralysis was due to the cooperative function between the tumor suppressors TRP53 and PTEN. Since this is out of the scope of this paper, we did not pursue further what caused the paralysis of hind limbs in 53PR mice.

DISCUSSION

It is well known that most human cancers result from the accumulation of multiple genetic changes, including activating mutations in oncogenes and the loss of function mutations in TSGs [55]. To understand the molecular mechanism of pituitary and pancreatic islet tumorigenesis, this paper and our recently published paper [48] together present a systematic evaluation of genetic interactions between the tissue-specific loss of common TSGs—*Rb1*, *Trp53*, *Pten*, and *Men1*—in mice. TSGs were deleted in pituitary and pancreatic islets using the Cre-LoxP system with Cre under the control of the rat insulin II promoter. Our systematic pairwise homozygous deletions of the TSGs directly illustrated the genetic interactions of these TSGs in suppressing PitNETs and PanNETs (Figure 9). Our data demonstrated that pRB had the strongest cooperative function with PTEN in suppressing PitNETs. pRB had strong cooperative function with TRP53 and Menin, respectively, in suppressing PitNETs and PanNETs. TRP53 had weak cooperative function with PTEN in suppressing pituitary growth. We also demonstrated that deletion of *Pten* singly led to prolactinomas in female mice and slow growth of the intermediate lobe of pituitaries in both female and male mice. Deletion of *Rb1* alone led to islet hyperplasia in pancreas and *Trp53* may play a role mainly in the intermediate lobe of the pituitary.

The genetic analysis of the tumorigenic phenotypes in single and double deletions of TSGs in pituitary implied that the order of functional importance of TSGs from most to least in pituitary tumorigenesis was *Rb1*, *Pten*, *Men1*, and *Trp53*. Mice with single deletion of *Rb1* using the RIP-Cre system developed fully penetrant ACTH-secreting PitNETs in our study, which is consistent with previous reports on heterozygous $Rb1^{+/-}$ mice [56]. Mice with single deletion of *Pten* in this study and *Men1* [37] developed prolactinomas, mainly in female mice at a latency. Mice with single deletion of *Trp53* did not develop PitNETs. These results indicate that deletion of *Rb1* had the strongest effect on the pituitary tumorigenesis.

M”1”RbRC mice developed PitNETs faster and more severely than MRb”1”RC mice further supporting a more important role for *Rb1* than *Men1*. Survival, pathology and phenotype of M”1”PRC and MP”1”RC mice showed that M”1”PRC mice developed PitNETs faster than MP”1”RC

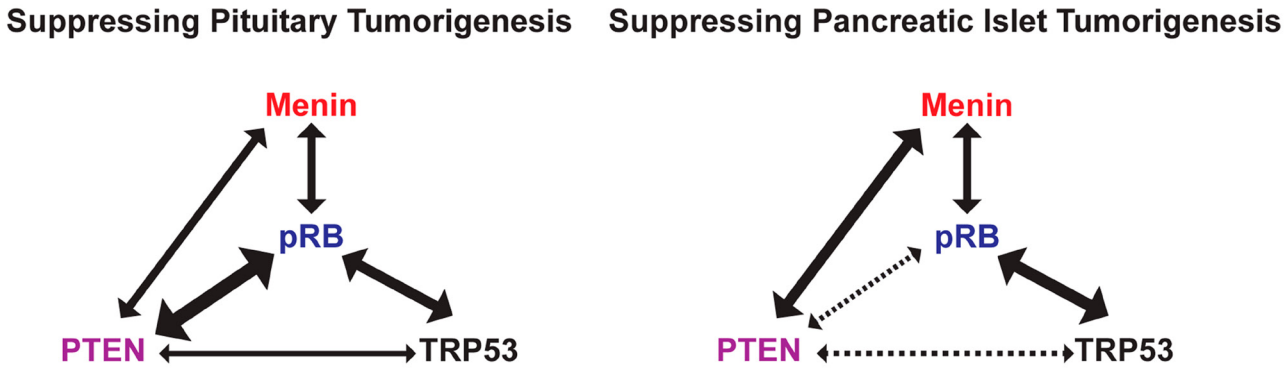

Figure 9: Genetic interactions between TSGs in suppressing pituitary and pancreatic islet tumorigenesis. Thick solid lines with double arrows meant the strong cooperative interaction; thin solid lines with double arrows meant the weak cooperative interaction; dotted lines with double arrows meant that cooperative interactions were not be able to be determined in this study; no lines meant no cooperative interaction.

mice, indicating that deletion of *Pten* had stronger effect on the development of PitNETs than deletion of *Men1*, and *Pten* played a more important role in pituitary tumorigenesis than *Men1*. Consistent with the important roles of *Rb1* and *Pten* in pituitary tumorigenesis, PRbR mice developed fully penetrant PitNETs the earliest at around six weeks of age. Although deletion of *Trp53* itself did not lead to PitNETs, double deletions with *Rb1* led to fully penetrant ACTH-secreting PitNETs by nine weeks, and double deletions with *Pten* led to slowly growing pituitaries with high serum ACTH concentrations, suggesting that *Trp53* played a role in pituitary tumorigenesis, perhaps mainly in the intermediate lobe of the pituitary. Given the fundamental difference in murine versus humans where ACTH corticotrophs are largely found in the anterior pituitary in humans and in the intermediate lobe in mice, it might be expected that *p53* mutations in humans would associate with anterior pituitary tumors.

Based on the age of onset and the rate of growth of tumors, we propose that deletion of *Rb1* affects the initiation and progression of pituitary tumorigenesis, deletion of *Pten* or of *Men1* has more of an effect on initiation than progression of pituitary tumorigenesis, while deletion of *Trp53* influences progression rather than initiation of pituitary tumorigenesis. Further characterization of multistep tumorigenesis and complex molecular signatures involved in pituitary tumorigenesis could be investigated through global transcriptional profiling of the PitNETs from these mice. Dissection of the molecular signatures involved in the pituitary tumorigenesis will help unravel molecular mechanisms. Collectively, pRB and PTEN/PI3K/AKT pathways play important roles in suppressing PitNETs in mice.

It is widely known that *MEN1* plays an important role in human PanNETs than other TSGs *RB1*, *TP53*, and *PTEN* based on genetic and genomic analysis of the human PanNETs. Here we performed targeted deletions of these four TSGs singly and pairwise in pancreatic islets in mice and demonstrated directly that deletion of *Men1* had the strongest effect on islet tumorigenesis, consistent with what is widely accepted in man. At fifteen weeks, MR mice did not show significant difference in the ratio of islets area per pancreas area from PR mice, but both MR and PR mice showed significantly larger islets area per pancreas area compared with RbR mice (Figure 3D), suggesting that deletion *Men1* or *Pten* had stronger effects on islet hyperplasia than deletion of *Rb1*. MR mice developed PanNETs after twenty-three weeks and with high frequency and severity increasing after thirty-five weeks (our study and [37]). Evaluation of islets area per pancreas area in M"1"PRC and MP"1"RC mice showed that MP"1"RC mice had significantly larger islets area per pancreas area compared to M"1"PRC mice at fifteen weeks (Figure 8H), supporting a more important role for Menin in islet tumorigenesis than PTEN.

Double homozygous deletions of *Men1* and *Pten* accelerated fully penetrant PanNETs [48] while double homozygous deletions of *Men1* and *Rb1* accelerated development of PanNETs in around 50% of mice, supporting a more important role for PTEN in islet tumorigenesis than pRb. Two possibilities could explain the function of pRb in islet lesions. One is that pRb and Menin may have some overlapping function in suppressing PanNETs. The other is that pRb has limited function in islet lesions. Due to PitNET development and death in RbR and MRbR mice, pancreas could not be examined at later time points. Using a different promoter with our experimental system would help address this question. Deletion of *Rb1* alone and in combination with *Men1* in mice containing the Cre transgene driven by the mouse insulin 1 promoter (MIP-Cre) [48] would lead to deletion of TSGs in pancreatic islets only. This would help us examine whether *Rb1* plays a role in islet tumorigenesis and whether *Men1* and *Rb1* have any overlapping function in islet tumorigenesis.

In this RIP-Cre system, pancreas sections from PRbR and 53PR mice were not evaluated at later time points due to early death in PRbR mice and hind limb paralysis in 53PR mice. Mice with double homozygous deletions of TSGs in pancreatic islets only using MIP-Cre system would help us understand whether double deficiencies of *Pten* with *Rb1* or *Trp53* have any cooperative tumorigenic effects on pancreatic islets. Double homozygous deletions of *Rb1* and *Men1* developed WD G1/G2 PanNETs while double homozygous deletions of *Rb1* and *Trp53* developed WD G3 PanNETs and double homozygous deletions of *Men1* and *Trp53* did not show a synergistic effect on islet tumorigenesis, as reported earlier [54]. These results indicate that even if Menin and pRb or Menin and TRP53 has overlapping functions in suppressing PanNETs, they also have mutually exclusive and independent functions in pancreatic islets.

Taken together, the order of functional importance of TSGs in islet tumorigenesis from most to least important is *Men1*, *Pten*, *Rb1*, and *Trp53*. Based on the age of onset, frequency and severity of tumorigenesis, we propose that deletion of *Men1* may affect more on initiation than progression of islet tumorigenesis, deletion of *Rb1* or of *Pten* may affect initiation of islet tumorigenesis, while deletion of *Trp53* may affect the progression of islet tumorigenesis. Menin and PTEN/PI3K/AKT pathways play important roles in suppressing PanNETs in mice.

In summary, our data clearly demonstrate that TSGs *Rb1*, *Pten*, *Men1*, and *Trp53* have distinct tissue specificity in neuroendocrine tumorigenesis in mouse and likely in man. The mouse models here and deletion of these TSGs in MIP-Cre mice will help further our understanding the molecular function of these TSGs and their pathways in PitNET and PanNET pathogenesis, which will help develop targeted novel therapeutic options in treating human patients.

MATERIALS AND METHODS

Genetic crosses and molecular analysis

To generate compound mice *Men1*$^{flox/flox}$ *Rb1*$^{flox/flox}$ RIP-Cre (MRbR) (Figure 1A), *Men1*$^{flox/flox}$ mice (129S (FVB)-*Men1*$^{tm1.2Cre}$/J, stock number 005109, The Jackson Laboratory, USA) were first crossed with *Rb1*$^{flox/flox}$ mice (FVB;129-*Rb1*^{tm2Brn}/Nci, stock number: 01XC1, The Frederick National Laboratory for Cancer Research, USA) to generate heterozygous *Men1*$^{+/flox}$ *Rb1*$^{+/flox}$ mice. The resulting mice were then intercrossed to generate *Men1*$^{flox/flox}$ *Rb1*$^{flox/flox}$ (MRb) mice. The resulting double homozygous floxed mice were then crossed with RIP-Cre mice (C57BL/6-Tg (Ins2-cre) 25Mgn/J, stock number: 003573, The Jackson Laboratory, USA) to generate *Men1*$^{+/flox}$ *Rb1*$^{+/flox}$ RIP-Cre mice. These mice were further crossed back to MRb mice to generate the desired double homozygous deletions MRbR compound mice, and corresponding littermates MRb, *Men1*$^{flox/+}$ *Rb1*$^{flox/flox}$ RIP-Cre (M"1"RbRC), *Men1*$^{flox/flox}$ *Rb1*$^{flox/+}$ RIP-Cre (MRb"1"RC), *Men1*$^{flox/+}$ *Rb1*$^{flox/+}$ RIP-Cre (M"1"Rb"1"RC). Confirmation of the genotypes in mice was evaluated by PCR using tail genomic DNA (Figure 1B). Tissue-specific expression of RIP-Cre in pancreatic islets and brain was confirmed previously [48]. Due to PitNETs developed in MRbR mice, MRbR mice were infertile. All of the MRbR mice and their littermates were generated through the series of crosses. Compound mice *Pten*$^{flox/flox}$ *Rb1*$^{flox/flox}$ RIP-Cre (PRbR), *Trp53*$^{flox/flox}$ *Pten*$^{flox/flox}$ RIP-Cre (53PR) and *Trp53*$^{flox/flox}$ *Rb1*$^{flox/flox}$ RIP-Cre (53RbR) were generated using the same strategy as for MRbR mice, except that *Pten*$^{flox/flox}$ mice (C;129S4-*Pten*^{tm1Hwu}/J, stock number: 004597, The Jackson Laboratory, USA) or/and *Trp53*$^{flox/flox}$ mice (B6.129P2-*Trp53*^{tm1Brn}/J, stock number: 008462, The Jackson Laboratory, USA) were used (Figure 7A and Supplementary Figure 1A). Confirmation of the genotypes in mice was evaluated by PCR using tail genomic DNA (Figure 7B and Supplementary Figure 1B and 1C). All of the PRbR, 53PR, 53RbR mice and their littermates were generated through the series of crosses due to sickness of these mice. The first generation of *Trp53*$^{flox/flox}$ *Men1*$^{flox/flox}$ RIP-Cre (53MR) mice was generated using the same strategy. Then 53 MR mice were crossed with each other to generate cohorts of 53MR mice and confirmation of the genotypes was evaluated by PCR using tail DNA (Supplementary Figure 1D). *Men1*$^{flox/+}$ *Pten*$^{flox/flox}$ RIP-Cre (M"1"PRC), *Men1*$^{flox/flox}$ *Pten*$^{flox/+}$ RIP-Cre (MP"1"RC) and *Men1*$^{flox/+}$ *Pten*$^{flox/+}$ RIP-Cre (M"1"P"1"RC) mice were the littermates from the crosses to generate *Men1*$^{flox/flox}$ *Pten*$^{flox/flox}$ RIP-Cre (MPR) mice [48]. Single deletion *Rb1*$^{flox/flox}$ RIP-Cre (RbR) mice were produced by generating heterozygous *Rb1*$^{+/flox}$ RIP-Cre animals through the first cross of *Rb1*$^{flox/flox}$ mice with RIP-Cre mice and then crossing the resulting *Rb1*$^{+/flox}$ RIP-Cre mice with *Rb1*$^{flox/flox}$ mice. Single deletion *Trp53*$^{flox/flox}$ RIP-Cre (53R), *Pten*$^{flox/flox}$ RIP-Cre (PR) and *Men1*$^{flox/flox}$ RIP-Cre (MR) mice were produced through a strategy similar to that used to produce RbR mice. All cohorts were in a mixed genetic background. Animals were housed in a temperature-, humidity-, and light-controlled room (12-hour light/dark cycle) and with free access to food and water. All animal experiments were conducted according to the research guidelines set forth by the Institutional Animal Care and Use Committee (IACUC) of Rutgers, the State University of New Jersey, USA.

Animals were genotyped by standard genomic PCR techniques using tail DNA. Tail Genomic DNA was isolated using Promega Nuclei Lysis solution/EDTA (Promega Corporation, USA). Primers for PCR analysis were ordered from Integrated DNA Technologies (IDT) based on Vendors' recommendations [57] (Table 4). PCR fragments from tail genomic DNA were amplified using a thermal cycler (Veriti, the applied biosystems, USA) (94°C, 3 min; 94°C, 30 sec, 60°C, 1 min, 72°C, 1 min, for 40 cycles; 72°C, 7 min, or as Vendor's recommendations).

Macroscopic and microscopic evaluation of pituitary and pancreas

This was basically performed the same as what described in [48]. To evaluate pituitary size inside the brain skull macroscopically, a ruler was used to measure the length, width and height of the pituitary at autopsy. The volume of a pituitary was calculated with the formula $V=(\pi/6) \times (\text{length} \times \text{width} \times \text{height})$. To evaluate pituitary histology, the brain skull with intact pituitary was fixed in 10% buffered formalin solution (Fisher Scientific, Inc., USA) for 48 h at 4°C. After fixation, pituitary was removed from the brain skull gently and wrapped inside a biopsy paper, then washed in 50% ethanol and transferred to 70% ethanol for paraffin embedding, further sectioned and stained in the immunohistochemistry experiments as described previously. Pancreas was examined from head to tail if there are any nodules/tumors macroscopically. To score PanNETs microscopically, three or four pancreas sections were sectioned 120 μm-apart from each mouse and stained with hematoxylin and eosin (H & E), insulin and glucagon. One or more islets of ≥ 1 mm in diameter in any of the three or four sections with positive insulin staining were scored as tumor for that mouse based on histologic examination. To evaluate islet lesions quantitatively, the insulin-stained pancreas sections from the three or four sections taken 120 μm-apart per mouse were digitized at 20 ×. The ratio of islets area (insulin positive area) per pancreas area for each mouse was calculated and graphed as described in [48]. For quantification of IHC positive staining for Ki-67, the areas with the highest density of Ki-67 reactivity among tumor cells were first identified. At least 1000 cells were counted at 20× magnification in these high Ki-67 density areas in a minimum of three mice. Antibodies used for

Table 4: List of primer sequences for genotyping

Gene Name	Primer Name	Primer sequences
Cre	oIMR1084	5′-GCG GTC TGG CAG TAA AAA CTA TC-3′
	oIMR1085	5′-GTG AAA CAG CAT TGC TGT CAC TT-3′
	oIMR7338	5′-CTA GGC CAC AGA ATT GAA AGA TCT-3′
	oIMR7339	5′-GTA GGT GGA AAT TCT AGC ATC ATC C-3′
Men1	oIMR1484	5′-CCC ACA TCC AGT CCC TCT TCA GCT-3′
	oIMR1485	5′-CCC TCT GGC TAT TCA ATG GCA GGG-3′
	primer C-R	5′-CGG AGA AAG AGG TAA TGA AAT GGC-3′
Rb1	R007	5′-GGC GTG TGC CAT CAA TG-3′
	R008	5′-AAC TCA AGG GAG ACC TG-3′
Pten	oIMR9554	5′-CAA GCA CTC TGC GAA CTG AG-3′
	oIMR9555	5′-AAG TTT TTG AAG GCA AGA TGC-3′
Trp53	oIMR8543	5′-GGT TAA ACC CAG CTT GAC CA-3′
	oIMR8544	5′-GGA GGC AGA GAC AGT TGG AG-3′

immunohistochemistry experiments were the same as described in [48].

Serum assays

All mice were fasted for 3–5 hours in the morning before blood collection. Blood glucose was measured with the ONE TOUCH Ultra2 blood glucose meter (Lifescan, Inc., USA). Serum insulin levels were measured with the Ultra Sensitive Mouse Insulin ELISA kit (Crystal Chem Inc., 90080, USA). Serum prolactin, growth hormone and ACTH levels were determined with the kits from Calbiotech (PR063F-100, USA), Millipore (EZRMGH-45K, USA) and Abcam Inc. (ab263880, USA), respectively. All experiments were performed based on manufacturers' instructions and repeated at least twice independently.

Statistical analysis

All statistical analyses and graphs were performed using GraphPad Prism version 6.0b software. The statistical significance of survival curves between two groups was analyzed using the log-rank (Mantel–Cox) test, and the statistical significance of serum hormone levels, of the ratio of islet area per pancreas area, of volume of pituitaries at death between two groups was analyzed using the unpaired *t*-test with Welch's correction. $p < 0.05$ was considered significant.

Abbreviations

TSGs: Tumor suppressor genes; *MEN1* or *Men1*: Multiple endocrine neoplasia type 1; PTEN or *Pten*: Phosphatase and tensin homolog; pRB or *Rb1*: retinoblastoma susceptibility gene 1; NETs: neuroendocrine tumors; PitNETs: pituitary neuroendocrine tumors; PanNETs: pancreatic neuroendocrine tumors; GH: growth hormone; ACTH: adrenocorticotropin hormone; MRbR: $Men1^{flox/flox}$ $Rb1^{flox/flox}$ RIP-Cre; MRb: $Men1^{flox/flox}$ $Rb1^{flox/flox}$; MR: $Men1^{flox/flox}$ RIP-Cre; RbR: $Rb1^{flox/flox}$ RIP-Cre; M"1"RbRC: $Men1^{flox/+}$ $Rb1^{flox/flox}$ RIP-Cre; MRb"1"RC: $Men1^{flox/flox}$ $Rb1^{flox/+}$ RIP-Cre; M"1"Rb"1"RC: $Men1^{flox/+}$ $Rb1^{flox/+}$ RIP-Cre; PR: $Pten^{flox/flox}$ RIP-Cre; P: $Pten^{flox/flox}$; MPR: $Men1^{flox/flox}$ $Pten^{flox/flox}$ RIP-Cre; M"1"PRC: $Men1^{flox/+}$ $Pten^{flox/flox}$ RIP-Cre; MP"1"RC: $Men1^{flox/flox}$ $Pten^{flox/+}$ RIP-Cre; M"1"P"1"RC: $Men1^{flox/+}$ $Pten^{flox/+}$ RIP-Cre; PRbR: $Pten^{flox/flox}$ $Rb1^{flox/flox}$ RIP-Cre; PRb: $Pten^{flox/flox}$ $Rb1^{flox/flox}$; 53RbR: $Trp53^{flox/flox}$ $Rb1^{flox/flox}$ RIP-Cre; 53R: $Trp53^{flox/flox}$ RIP-Cre; 53Rb: $Trp53^{flox/flox}$ $Rb1^{flox/flox}$; 53PR: $Trp53^{flox/flox}$ $Pten^{flox/flox}$ RIP-Cre; 53MR: $Trp53^{flox/flox}$ $Men1^{flox/flox}$ RIP-Cre.

ACKNOWLEDGMENTS

We sincerely thank Dr. Arnold J. Levine for his invaluable discussions and suggestions throughout the project and contributing reagents. We would also like to thank Richard Clausen for breeding the mice and performing genotyping for the project, the Raymond and Beverly Sackler Foundation and Princeton University for their support of our research, and Histopathology Services and the Biomedical Imaging shared resources of Rutgers Cancer Institute of New Jersey for their help.

CONFLICTS OF INTEREST

The authors declare no potential conflicts of interest.

FUNDING

Research reported in this publication was supported in part by the National Center for Advancing Translational

Sciences (NCATS), a component of the National Institute of Health (NIH) under award number UL1TR003017.

REFERENCES

1. Newey PJ, Gorvin CM, Cleland SJ, Willberg CB, Bridge M, Azharuddin M, Drummond RS, van der Merwe PA, Klenerman P, Bountra C, Thakker RV. Mutant prolactin receptor and familial hyperprolactinemia. N Engl J Med. 2013; 369:2012–2020. https://doi.org/10.1056/NEJMoa1307557. [PubMed]
2. Ezzat S, Asa SL, Couldwell WT, Barr CE, Dodge WE, Vance ML, McCutcheon IE. The prevalence of pituitary adenomas: a systematic review. Cancer. 2004; 101:613–619. https://doi.org/10.1002/cncr.20412. [PubMed]
3. Melmed S. Pathogenesis of pituitary tumors. Nat Rev Endocrinol. 2011; 7:257–266. https://doi.org/10.1038/nrendo.2011.40. [PubMed]
4. Evans CO, Young AN, Brown MR, Brat DJ, Parks JS, Neish AS, Oyesiku NM. Novel patterns of gene expression in pituitary adenomas identified by complementary deoxyribonucleic acid microarrays and quantitative reverse transcription-polymerase chain reaction. J Clin Endocrinol Metab. 2001; 86:3097–3107. https://doi.org/10.1210/jcem.86.7.7616. [PubMed]
5. Aflorei ED, Korbonits M. Epidemiology and etiopathogenesis of pituitary adenomas. J Neurooncol. 2014; 117:379–394. https://doi.org/10.1007/s11060-013-1354-5. [PubMed]
6. Daly AF, Rixhon M, Adam C, Dempegioti A, Tichomirowa MA, Beckers A. High prevalence of pituitary adenomas: a cross-sectional study in the province of Liege, Belgium. J Clin Endocrinol Metab. 2006; 91:4769–4775. https://doi.org/10.1210/jc.2006-1668. [PubMed]
7. Raappana A, Koivukangas J, Ebeling T, Pirila T. Incidence of pituitary adenomas in Northern Finland in 1992–2007. J Clin Endocrinol Metab. 2010; 95:4268–4275. https://doi.org/10.1210/jc.2010-0537. [PubMed]
8. Bosman FT, Carneiro F, Hruban RH, Theise ND. World Health Organization (WHO) Classification of Tumours of the Digestive System. Lyon, France: IARC Press; 2010.
9. Rindi G, Klersy C, Albarello L, Baudin E, Bianchi A, Buchler MW, Caplin M, Couvelard A, Cros J, de Herder WW, Delle Fave G, Doglioni C, Federspiel B, et al. Competitive Testing of the WHO 2010 versus the WHO 2017 Grading of Pancreatic Neuroendocrine Neoplasms: Data from a Large International Cohort Study. Neuroendocrinology. 2018; 107:375–386. https://doi.org/10.1159/000494355. [PubMed]
10. Sigel CS, Krauss Silva VW, Reid MD, Chhieng D, Basturk O, Sigel KM, Daniel TD, Klimstra DS, Tang LH. Assessment of cytologic differentiation in high-grade pancreatic neuroendocrine neoplasms: A multi-institutional study. Cancer Cytopathol. 2018; 126:44–53. https://doi.org/10.1002/cncy.21934. [PubMed]
11. Liu E, Marincola P, Oberg K. Everolimus in the treatment of patients with advanced pancreatic neuroendocrine tumors: latest findings and interpretations. Therap Adv Gastroenterol. 2013; 6:412–419. https://doi.org/10.1177/1756283X13496970. [PubMed]
12. Tang LH, Basturk O, Sue JJ, Klimstra DS. A Practical Approach to the Classification of WHO Grade 3 (G3) Well-differentiated Neuroendocrine Tumor (WD-NET) and Poorly Differentiated Neuroendocrine Carcinoma (PD-NEC) of the Pancreas. Am J Surg Pathol. 2016; 40:1192–1202. https://doi.org/10.1097/PAS.0000000000000662. [PubMed]
13. Knudson AG Jr. Mutation and cancer: statistical study of retinoblastoma. Proc Natl Acad Sci U S A. 1971; 68:820–823. https://doi.org/10.1073/pnas.68.4.820. [PubMed]
14. Olivier M, Hollstein M, Hainaut P. TP53 mutations in human cancers: origins, consequences, and clinical use. Cold Spring Harb Perspect Biol. 2010; 2:a001008. https://doi.org/10.1101/cshperspect.a001008. [PubMed]
15. Soussi T. TP53 mutations in human cancer: database reassessment and prospects for the next decade. Adv Cancer Res. 2011; 110:107–139. https://doi.org/10.1016/B978-0-12-386469-7.00005-0. [PubMed]
16. Nevins JR. The Rb/E2F pathway and cancer. Hum Mol Genet. 2001; 10:699–703. https://doi.org/10.1093/hmg/10.7.699. [PubMed]
17. Cryns VL, Alexander JM, Klibanski A, Arnold A. The retinoblastoma gene in human pituitary tumors. J Clin Endocrinol Metab. 1993; 77:644–646. https://doi.org/10.1210/jcem.77.3.7690360. [PubMed]
18. Ikeda H, Yoshimoto T, Shida N. Molecular analysis of p21 and p27 genes in human pituitary adenomas. Br J Cancer. 1997; 76:1119–1123. https://doi.org/10.1038/bjc.1997.521. [PubMed]
19. Jaffrain-Rea ML, Ferretti E, Toniato E, Cannita K, Santoro A, Di Stefano D, Ricevuto E, Maroder M, Tamburrano G, Cantore G, Gulino A, Martinotti S. p16 (INK4a, MTS-1) gene polymorphism and methylation status in human pituitary tumours. Clin Endocrinol (Oxf). 1999; 51:317–325. https://doi.org/10.1046/j.1365-2265.1999.00774.x. [PubMed]
20. Takeuchi S, Koeffler HP, Hinton DR, Miyoshi I, Melmed S, Shimon I. Mutation and expression analysis of the cyclin-dependent kinase inhibitor gene p27/Kip1 in pituitary tumors. J Endocrinol. 1998; 157:337–341. https://doi.org/10.1677/joe.0.1570337. [PubMed]
21. Herman V, Drazin NZ, Gonsky R, Melmed S. Molecular screening of pituitary adenomas for gene mutations and rearrangements. J Clin Endocrinol Metab. 1993; 77:50–55. https://doi.org/10.1210/jcem.77.1.8100831. [PubMed]
22. Levy A, Hall L, Yeudall WA, Lightman SL. p53 gene mutations in pituitary adenomas: rare events. Clin Endocrinol (Oxf). 1994; 41:809–814. https://doi.org/10.1111/j.1365-2265.1994.tb02797.x. [PubMed]

23. Tanizaki Y, Jin L, Scheithauer BW, Kovacs K, Roncaroli F, Lloyd RV. P53 gene mutations in pituitary carcinomas. Endocr Pathol. 2007; 18:217–222. https://doi.org/10.1007/s12022-007-9006-y. [PubMed]
24. Thapar K, Scheithauer BW, Kovacs K, Pernicone PJ, Laws ER Jr. p53 expression in pituitary adenomas and carcinomas: correlation with invasiveness and tumor growth fractions. Neurosurgery. 1996; 38:765–770, discussion 70–71. https://doi.org/10.1227/00006123-199604000-00027. [PubMed]
25. Ogino A, Yoshino A, Katayama Y, Watanabe T, Ota T, Komine C, Yokoyama T, Fukushima T. The p15(INK4b)/p16(INK4a)/RB1 pathway is frequently deregulated in human pituitary adenomas. J Neuropathol Exp Neurol. 2005; 64:398–403. https://doi.org/10.1093/jnen/64.5.398. [PubMed]
26. Yoshino A, Katayama Y, Ogino A, Watanabe T, Yachi K, Ohta T, Komine C, Yokoyama T, Fukushima T. Promoter hypermethylation profile of cell cycle regulator genes in pituitary adenomas. J Neurooncol. 2007; 83:153–162. https://doi.org/10.1007/s11060-006-9316-9. [PubMed]
27. Bates AS, Farrell WE, Bicknell EJ, McNicol AM, Talbot AJ, Broome JC, Perrett CW, Thakker RV, Clayton RN. Allelic deletion in pituitary adenomas reflects aggressive biological activity and has potential value as a prognostic marker. J Clin Endocrinol Metab. 1997; 82:818–824. https://doi.org/10.1210/jcem.82.3.3799. [PubMed]
28. Simpson DJ, Hibberts NA, McNicol AM, Clayton RN, Farrell WE. Loss of pRb expression in pituitary adenomas is associated with methylation of the RB1 CpG island. Cancer Res. 2000; 60:1211–1216. [PubMed]
29. Williams BO, Schmitt EM, Remington L, Bronson RT, Albert DM, Weinberg RA, Jacks T. Extensive contribution of Rb-deficient cells to adult chimeric mice with limited histopathological consequences. EMBO J. 1994; 13:4251–4259. https://doi.org/10.1002/j.1460-2075.1994.tb06745.x. [PubMed]
30. Hu N, Gutsmann A, Herbert DC, Bradley A, Lee WH, Lee EY. Heterozygous Rb-1 delta 20/+mice are predisposed to tumors of the pituitary gland with a nearly complete penetrance. Oncogene. 1994; 9:1021–1027. [PubMed]
31. Harvey M, Vogel H, Lee EY, Bradley A, Donehower LA. Mice deficient in both p53 and Rb develop tumors primarily of endocrine origin. Cancer Res. 1995; 55:1146–1151. [PubMed]
32. Glenn ST, Jones CA, Sexton S, LeVea CM, Caraker SM, Hajduczok G, Gross KW. Conditional deletion of p53 and Rb in the renin-expressing compartment of the pancreas leads to a highly penetrant metastatic pancreatic neuroendocrine carcinoma. Oncogene. 2014; 33:5706–5715. https://doi.org/10.1038/onc.2013.514. [PubMed]
33. Gaudray P, Weber G. Genetic background of MEN1: from genetic homogeneity to functional diversity. Adv Exp Med Biol. 2009; 668:17–26. https://doi.org/10.1007/978-1-4419-1664-8_2. [PubMed]
34. Thakker RV. Multiple endocrine neoplasia. Horm Res. 2001; 56:67–72. https://doi.org/10.1159/000048138. [PubMed]
35. Jiao Y, Shi C, Edil BH, de Wilde RF, Klimstra DS, Maitra A, Schulick RD, Tang LH, Wolfgang CL, Choti MA, Velculescu VE, Diaz LA, Jr, Vogelstein B, et al. DAXX/ATRX, MEN1, and mTOR pathway genes are frequently altered in pancreatic neuroendocrine tumors. Science. 2011; 331:1199–1203. https://doi.org/10.1126/science.1200609. [PubMed]
36. Scarpa A, Chang DK, Nones K, Corbo V, Patch AM, Bailey P, Lawlor RT, Johns AL, Miller DK, Mafficini A, Rusev B, Scardoni M, Antonello D, et al, and Australian Pancreatic Cancer Genome Initiative. Whole-genome landscape of pancreatic neuroendocrine tumours. Nature. 2017; 543:65–71. https://doi.org/10.1038/nature21063. [PubMed]
37. Crabtree JS, Scacheri PC, Ward JM, McNally SR, Swain GP, Montagna C, Hager JH, Hanahan D, Edlund H, Magnuson MA, Garrett-Beal L, Burns AL, Ried T, et al. Of mice and MEN1: Insulinomas in a conditional mouse knockout. Mol Cell Biol. 2003; 23:6075–6085. https://doi.org/10.1128/MCB.23.17.6075-6085.2003. [PubMed]
38. Bertolino P, Tong WM, Galendo D, Wang ZQ, Zhang CX. Heterozygous Men1 mutant mice develop a range of endocrine tumors mimicking multiple endocrine neoplasia type 1. Mol Endocrinol. 2003; 17:1880–1892. https://doi.org/10.1210/me.2003-0154. [PubMed]
39. Biondi CA, Gartside MG, Waring P, Loffler KA, Stark MS, Magnuson MA, Kay GF, Hayward NK. Conditional inactivation of the MEN1 gene leads to pancreatic and pituitary tumorigenesis but does not affect normal development of these tissues. Mol Cell Biol. 2004; 24:3125–3131. https://doi.org/10.1128/MCB.24.8.3125-3131.2004. [PubMed]
40. Chung DC, Brown SB, Graeme-Cook F, Tillotson LG, Warshaw AL, Jensen RT, Arnold A. Localization of putative tumor suppressor loci by genome-wide allelotyping in human pancreatic endocrine tumors. Cancer Res. 1998; 58:3706–3711. [PubMed]
41. Rigaud G, Missiaglia E, Moore PS, Zamboni G, Falconi M, Talamini G, Pesci A, Baron A, Lissandrini D, Rindi G, Grigolato P, Pederzoli P, Scarpa A. High resolution allelotype of nonfunctional pancreatic endocrine tumors: identification of two molecular subgroups with clinical implications. Cancer Res. 2001; 61:285–292. [PubMed]
42. Perren A, Komminoth P, Saremaslani P, Matter C, Feurer S, Lees JA, Heitz PU, Eng C. Mutation and expression analyses reveal differential subcellular compartmentalization of PTEN in endocrine pancreatic tumors compared to normal islet cells. Am J Pathol. 2000; 157:1097–1103. https://doi.org/10.1016/S0002-9440(10)64624-X. [PubMed]
43. Lamberti G, Brighi N, Maggio I, Manuzzi L, Peterle C, Ambrosini V, Ricci C, Casadei R, Campana D. The Role of mTOR in Neuroendocrine Tumors: Future Cornerstone of a Winning Strategy? Int J Mol Sci. 2018; 19:747. https://doi.org/10.3390/ijms19030747. [PubMed]

44. Liu IH, Ford JM, Kunz PL. DNA-repair defects in pancreatic neuroendocrine tumors and potential clinical applications. Cancer Treat Rev. 2016; 44:1–9. https://doi.org/10.1016/j.ctrv.2015.11.006. [PubMed]

45. Chou WC, Lin PH, Yeh YC, Shyr YM, Fang WL, Wang SE, Liu CY, Chang PM, Chen MH, Hung YP, Li CP, Chao Y, Chen MH. Genes involved in angiogenesis and mTOR pathways are frequently mutated in Asian patients with pancreatic neuroendocrine tumors. Int J Biol Sci. 2016; 12:1523–1532. https://doi.org/10.7150/ijbs.16233. [PubMed]

46. Tena-Suck ML, Ortiz-Plata A, de la Vega HA. Phosphatase and tensin homologue and pituitary tumor-transforming gene in pituitary adenomas. Clinical-pathologic and immunohistochemical analysis. Ann Diagn Pathol. 2008; 12:275–282. https://doi.org/10.1016/j.anndiagpath.2008.02.001. [PubMed]

47. Cakir M, Grossman AB. Targeting MAPK (Ras/ERK) and PI3K/Akt pathways in pituitary tumorigenesis. Expert Opin Ther Targets. 2009; 13:1121–1134. https://doi.org/10.1517/14728220903170675. [PubMed]

48. Wong C, Tang LH, Davidson C, Vosburgh E, Chen W, Foran DJ, Notterman DA, Levine AJ, Xu EY. Two well-differentiated pancreatic neuroendocrine tumor mouse models. Cell Death Differ. 2020; 27:269–283. https://doi.org/10.1038/s41418-019-0355-0. [PubMed]

49. Bai F, Pei XH, Pandolfi PP, Xiong Y. p18 Ink4c and Pten constrain a positive regulatory loop between cell growth and cell cycle control. Mol Cell Biol. 2006; 26:4564–4576. https://doi.org/10.1128/MCB.00266-06. [PubMed]

50. Loffler KA, Biondi CA, Gartside MG, Serewko-Auret MM, Duncan R, Tonks ID, Mould AW, Waring P, Muller HK, Kay GF, Hayward NK. Lack of augmentation of tumor spectrum or severity in dual heterozygous Men1 and Rb1 knockout mice. Oncogene. 2007; 26:4009–4017. https://doi.org/10.1038/sj.onc.1210163. [PubMed]

51. Matoso A, Zhou Z, Hayama R, Flesken-Nikitin A, Nikitin AY. Cell lineage-specific interactions between Men1 and Rb in neuroendocrine neoplasia. Carcinogenesis. 2008; 29:620–628. https://doi.org/10.1093/carcin/bgm207. [PubMed]

52. Jarskar R. Electron microscopical study on the development of the nerve supply of the pituitary pars intermedia of the mouse. Cell Tissue Res. 1977; 184:121–132. https://doi.org/10.1007/BF00220532. [PubMed]

53. Jacks T, Fazeli A, Schmitt EM, Bronson RT, Goodell MA, Weinberg RA. Effects of an Rb mutation in the mouse. Nature. 1992; 359:295–300. https://doi.org/10.1038/359295a0. [PubMed]

54. Loffler KA, Mould AW, Waring PM, Hayward NK, Kay GF. Menin and p53 have non-synergistic effects on tumorigenesis in mice. BMC Cancer. 2012; 12:252. https://doi.org/10.1186/1471-2407-12-252. [PubMed]

55. Vogelstein B, Kinzler KW. The multistep nature of cancer. Trends Genet. 1993; 9:138–141. https://doi.org/10.1016/0168-9525(93)90209-Z. [PubMed]

56. Nikitin AY, Juarez-Perez MI, Li S, Huang L, Lee WH. RB-mediated suppression of spontaneous multiple neuroendocrine neoplasia and lung metastases in Rb+/- mice. Proc Natl Acad Sci U S A. 1999; 96:3916–3921. https://doi.org/10.1073/pnas.96.7.3916. [PubMed]

57. Libutti SK, Crabtree JS, Lorang D, Burns AL, Mazzanti C, Hewitt SM, O'Connor S, Ward JM, Emmert-Buck MR, Remaley A, Miller M, Turner E, Alexander HR, et al. Parathyroid gland-specific deletion of the mouse Men1 gene results in parathyroid neoplasia and hypercalcemic hyperparathyroidism. Cancer Res. 2003; 63:8022–8028. [PubMed]

Cell Death & Differentiation (2020) 27:269–283
https://doi.org/10.1038/s41418-019-0355-0

Cell Death & Differentiation

ARTICLE

Two well-differentiated pancreatic neuroendocrine tumor mouse models

Chung Wong[1,11] · Laura H. Tang[2] · Christian Davidson[3] · Evan Vosburgh[1,4,5,12] · Wenjin Chen[4,6] · David J. Foran[4,6] · Daniel A. Notterman[7] · Arnold J. Levine[8] · Eugenia Y. Xu[1,4,9,10]

Received: 18 January 2019 / Revised: 26 April 2019 / Accepted: 7 May 2019 / Published online: 3 June 2019

Abstract

Multiple endocrine neoplasia type 1 (MEN1) is a genetic syndrome in which patients develop neuroendocrine tumors (NETs), including pancreatic neuroendocrine tumors (PanNETs). The prolonged latency of tumor development in MEN1 patients suggests a likelihood that other mutations cooperate with *Men1* to induce PanNETs. We propose that *Pten* loss combined with *Men1* loss accelerates tumorigenesis. To test this, we developed two genetically engineered mouse models (GEMMs)—MPR ($Men1^{flox/flox}$ $Pten^{flox/flox}$ RIP-Cre) and MPM ($Men1^{flox/flox}$ $Pten^{flox/flox}$ MIP-Cre) using the Cre-LoxP system with insulin-specific biallelic inactivation of *Men1* and *Pten*. Cre in the MPR mouse model was driven by the transgenic rat insulin 2 promoter while in the MPM mouse model was driven by the knock-in mouse insulin 1 promoter. Both mouse models developed well-differentiated (WD) G1/G2 PanNETs at a much shorter latency than *Men1* or *Pten* single deletion alone and exhibited histopathology of human MEN1-like tumor. The MPR model, additionally, developed pituitary neuroendocrine tumors (PitNETs) in the same mouse at a much shorter latency than *Men1* or *Pten* single deletion alone as well. Our data also demonstrate that Pten plays a role in NE tumorigenesis in pancreas and pituitary. Treatment with the mTOR inhibitor rapamycin delayed the growth of PanNETs in both MPR and MPM mice, as well as the growth of PitNETs, resulting in prolonged survival in MPR mice. Our MPR and MPM mouse models are the first to underscore the cooperative roles of *Men1* and *Pten* in cancer, particularly neuroendocrine cancer. The early onset of WD PanNETs mimicking the human counterpart in MPR and MPM mice at 7 weeks provides an effective platform for evaluating therapeutic opportunities for NETs through targeting the MENIN-mediated and PI3K/AKT/mTOR signaling pathways.

Edited by G. Melino

Supplementary information The online version of this article (https://doi.org/10.1038/s41418-019-0355-0) contains supplementary material, which is available to authorized users.

✉ Eugenia Y. Xu
exu@princeton.edu

[1] Raymond and Beverly Sackler Foundation Laboratory, New Brunswick, NJ 08901, USA

[2] Department of Pathology, Memorial Sloan-Kettering Cancer Center, New York, NY 10065, USA

[3] Department of Pathology, University of Utah, Huntsman Cancer Institute, Salt Lake City, UT 84112, USA

[4] Rutgers Cancer Institute of New Jersey, Rutgers, the State University of New Jersey, New Brunswick, NJ 08903, USA

[5] Department of Medicine, Robert Wood Johnson Medical School, Rutgers, the State University of New Jersey, New Brunswick, NJ 08901, USA

[6] Department of Pathology and Laboratory Medicine, Robert Wood Johnson Medical School, Rutgers, the State University of New Jersey, New Brunswick, NJ 08901, USA

[7] Department of Molecular Biology, Princeton University, Princeton, NJ 08544, USA

[8] School of Natural Sciences, Institute for Advanced Study, Princeton, NJ 08540, USA

[9] Department of Pediatrics, Robert Wood Johnson Medical School, Rutgers, the State University of New Jersey, New Brunswick, NJ 08901, USA

[10] Present address: Department of Molecular Biology, Princeton University, Princeton, NJ 08544, USA

[11] Present address: Regeneron Inc., Tarrytown, NY 10591, USA

[12] Present address: Department of Medicine, Yale University School of Medicine, New Haven, CT 06510, USA

Introduction

Neuroendocrine tumors (NETs) constitute a heterogeneous group of neoplasms that can arise from the NE cells found

in numerous tissues throughout the body including the gastroenteropancreatic tract, bronchopulmonary system, pituitary, parathyroids, thyroid, and ovaries. Pancreatic NETs (PanNETs) are found in the gastroenteropancreatic tract. Human pancreatic NE neoplasms are classified as either well-differentiated (WD) tumor (WD-NET) or poorly differentiated (PD) carcinoma (PD-NEC) [1]. WD PanNETs can be functional, secreting biologically active hormones such as insulin, glucagon, and others, or non-functional. PD-PanNECs are genetically and biologically related to conventional carcinoma with worse clinical prognosis [2]. Based on Ki 67 index, WD PanNETs are graded as G1 (<3%), G2 (3–20%), or G3 (>20%) [3, 4].

When surgery is not an option, the Food and Drug Administration has three approved drugs to treat progressive PanNETs: everolimus (rapamycin analog), sunitinib, and radiotherapy Lutathera (somatostatin analogs) [5–8]. The preclinical efficacy of rapamycin and sunitinib was demonstrated using the human BON-1 xenograft and RIP-Tag2 mouse models [9–13]. These mice develop PanNETs with poorly differentiated and high-grade histology, which do not resemble the counterpart of human PanNETs [14, 15]. Additional preclinical murine models that more closely reflect the histology and behavior of human WD PanNETs are needed.

Multiple endocrine neoplasia type 1 (MEN1) is an autosomal-dominant inherited syndrome with manifestation of NETs that involve at least two of the four endocrine glands, frequently parathyroid glands, endocrine pancreas, anterior pituitary, and adrenal gland [16–19]. The *MEN1* gene is responsible for the syndrome. Its gene product, MENIN, is a highly conserved tumor suppressor [20]. Biallelic inactivation of *MEN1* occurs in 44% of human PanNETs, inherited or sporadic, and is sufficient to drive tumorigenesis with long latency [21]. The delayed latency of NET development suggests that additional molecular and genetic events might be required for tumorigenesis.

The human and mouse genes share a highly conserved genomic structure with 89% nucleotide sequence homology and 97% amino acid sequence homology, respectively [22]. Mouse strains with defective *Men1* possess remarkable phenotypic and histological overlap with the human *MEN1* syndrome. Heterozygous *Men1* mice or homozygous β-cell-specific *Men1* deletion mice develop WD PanNETs and pituitary neuroendocrine tumors (PitNETs) also with long latency [23–28] as human MEN1 patients.

The tumorigenic latency in the Men1 mouse model makes it less ideal for the preclinical testing of candidate drugs. Identifying genes that function cooperatively with *Men1* could help us develop a better preclinical WD PanNET mouse model. In seeking targets, we consider the phosphoinositide 3-kinase (PI3K)/protein kinase B (AKT)/mammalian target of rapamycin (mTOR) signaling pathway, the second most mutated pathway in cancer, after p53 [29]. The mTOR pathway plays an important role in human NETs based on genome sequencing [21, 30–34]. Additionally, an mTOR inhibitor, everolimus, is used to treat PanNET patients. Phosphatase and tensin homolog (PTEN), a key negative regulator of the PI3K/AKT/mTOR pathway, is frequently mutated or lost in several familial or sporadic cancer types; however, in PanNETs, the frequency of loss is low, 7–26.4% [21, 32–38]. Co-mutations of *MEN1* and *PTEN* have been observed in a small percentage of human PanNETs [21, 32]. Thus we hypothesize that Menin and Pten may function cooperatively to suppress NE tumorigenesis.

Here we generated two genetically engineered mouse models (GEMMs) harboring homozygous deletions of *Men1* and *Pten* within insulin-producing β-cells and compared histopathology with the Men1 and Pten mouse models. Concomitant loss of *Pten* and *Men1* accelerated NE tumorigenesis. These GEMMs could provide improved preclinical therapeutic models for WD PanNET.

Methods and materials

Animals

To generate compound mice $Men1^{flox/flox}$ $Pten^{flox/flox}$ RIP-Cre (MPR) (Supplementary Fig. S1A), $Men1^{flox/flox}$ mice (129S (FVB)-$Men1^{tm1.2Ctre}$/J, stock number 005109, The Jackson Laboratory, USA) were first crossed with $Pten^{flox/flox}$ mice (C;129S4-$Pten^{tm1Hwu}$/J, stock number: 004597, The Jackson Laboratory, USA) to generate heterozygous $Men1^{+/flox}$ $Pten^{+/flox}$ mice. The resulting mice were then intercrossed to generate $Men1^{flox/flox}$ $Pten^{flox/flox}$ (MP) mice. The resulting homozygous mice were then crossed with RIP-Cre mice (C57BL/6-Tg(Ins2-cre) 25Mgn/J, stock number: 003573, The Jackson Laboratory, USA) to generate $Men1^{+/flox}$ $Pten^{+/flox}$ RIP-Cre mice. These mice were further crossed back to MP mice to generate the desired MPR compound mice and corresponding littermates MP. Confirmation of the genotypes in mice was evaluated by PCR using tail genomic DNA (Supplementary Fig. S1B). Tissue-specific deletion of *Men1* and/or *Pten* genes was confirmed by PCR using genomic DNA from various organs. Supplementary Fig. S1C showed that *Men1* and *Pten* genes were specifically deleted in pancreatic islets and brain, but not in heart, intestine, kidney, liver, lung, spleen, and pancreatic exocrine tissues in the representative MPR mice. This is consistent with the previous report that RIP-Cre is specifically expressed in pancreatic islets and hypothalamus [24, 39].

$Pten^{flox/flox}$ RIP-Cre (PR) mice were produced by generating heterozygous $Pten^{+/flox}$ RIP-Cre animals by the first

cross of *Pten*$^{flox/flox}$ mice with RIP-Cre mice, then by crossing the resulting *Pten*$^{+/flox}$ RIP-Cre mice with *Pten*$^{flox/flox}$ mice. *Men1*$^{flox/flox}$ RIP-Cre (MR) mice were produced similarly as the strategy to produce PR mice. The same strategy was taken to generate compound mice *Men1*$^{flox/flox}$ *Pten*$^{flox/flox}$ MIP-Cre (MPM), *Men1*$^{flox/flox}$ MIP-Cre (MM), and *Pten*$^{flox/flox}$ MIP-Cre (PM), except that MIP-Cre (B6 (Cg)-*Ins1*$^{tm1.1(cre)Thor}$/J, The Jackson Laboratory, USA) mice were used instead of RIP-Cre mice. To generate MPM, MM, and PM mice more quickly, first-generation MPM, MM, or PM mice were bred with MP, *Men1*$^{flox/flox}$, or *Pten*$^{flox/flox}$ mice, respectively, to obtain second-generation MPM, MM, or PM mice for the experiments. Animals were genotyped by using vendors' recommended primers (The Jackson Laboratory, USA) [40] and standard genomic PCR techniques. All cohorts were in a mixed genetic background. Animals were housed in a temperature-, humidity-, and light-controlled room (12-h light/dark cycle), allowing free access to food and water.

Mice were studied alongside age- and sex-matched control animals unless otherwise indicated.

All animal experiments were conducted according to the research guidelines set forth by the Institutional Animal Care and Use Committee (IACUC) of Rutgers, the State University of New Jersey, USA.

Evaluation of pituitary size

A ruler was used to measure the size of a pituitary at autopsy. The volume of a pituitary was calculated with the formula $V = (\pi/6) \times (\text{length} \times \text{width} \times \text{height})$. The dimensions of a normal pituitary are: 3–3.5 mm in length, 1–1.5 mm in width and depth.

Evaluation of PanNET formation

To score PanNETs, three 120-μm apart pancreas sections from each mouse were stained with hematoxylin and eosin (H & E), glucagon, and insulin. The sections were evaluated histologically. One or more islets of ≥1 mm in diameter with loss of α-cells (negative immunoreactivity for glucagon) and clonal proliferation of β-cells (positive immunoreactivity for insulin) in any of the three sections were considered as tumor development (PanNET) in that mouse.

Histology and immunohistochemistry (IHC)

Tissues were fixed in 10% buffered formalin solution (Fisher Scientific, Inc., USA) for 24 h at room temperature or for 48 h at 4 °C. Fixed tissues were then washed in 50% ethanol and transferred to 70% ethanol for paraffin embedding. For IHC, paraffin-embedded tissues were cut into 4-μm sections and stained with H&E. All IHC staining was performed on 4-μm paraffin-embedded sections and placed on charged glass slides. Sections were de-waxed with histoclear (National Diagnostics, Inc., USA) and rehydrated through graded alcohol. Antigen retrieval was then performed by incubating the slides in antigen retrieval solution (Vector Labs, USA) at 95 °C for 15 min. Slides were then allowed to cool for 20 min on ice. After washing in phosphate-buffered saline (PBS) with 0.1% Tween 20, the slides were blocked with a 3% hydrogen peroxide solution for 10 min. The slides were then washed in PBS with 0.1% Tween 20. The endogenous biotin activity was inactivated using the Endogenous Biotin Blocking Kit (Invitrogen, Inc., USA). The following detection and visualization procedures were performed according to the manufacturers' protocol. Slides were counterstained in Gill's hematoxylin, dehydrated, cleared, and cover-slipped. Negative control slides were run without primary antibody. Control slides known to be positive for each antibody were incorporated. DAKO antibodies (Fisher Scientific, USA): Insulin (A0564), Prolactin (A0569), and Growth hormone (GH) (A0570); Cell Signaling antibodies (Cell Signaling Technology Inc., Danvers, MA, USA): Glucagon (2760), Pten (9559); Abcam antibodies: Chromograinin A (ab15160), Ki 67 (ab15580), adrenocorticotropin hormone (ACTH) (ab74967); synaptophysin (Roche, 790-4407, USA); and Menin (Bethyl Lab, a300-105a) were used.

Proliferation index

For quantification of IHC positive staining for Ki 67, the areas with the highest density of Ki 67 reactivity among tumor cells were first identified. At least 1000 cells were counted at ×20 magnification in these high Ki 67 density areas in a minimum of three mice of each genotype and sex.

Ratio of the islets area per pancreas area

IHC-insulin-stained pancreas sections from three 120-μm apart sections per mouse (three or more samples of each genotype and sex were used) were digitized at ×20 at Rutgers Cancer Institute of New Jersey Biomedical Informatics shared resource using an Olympus VS120 whole slide scanner (Olympus Corporation of the Americas, Center Valley, PA). The image analysis algorithm was custom developed on Visiopharm image analysis platform (Visiopharm A/S, Hoersholm, Denmark). Insulin-positive pancreatic islets were digitally recognized and outlined. The diameter and area of individual islets were measured accordingly, and the area of the whole pancreas was measured as well. For quantitative analysis, the islets-to-pancreas ratio was calculated and graphed.

Molecular analysis

Genomic DNA was isolated using the QIAamp DNA Mini Kit (Qiagen, USA) and total RNA was isolated using the RNeasy Mini Kit (Qiagen, USA) per the manufacturer's instruction. PCR fragments from genomic DNA were amplified using a thermal cycler (Veriti, the Applied Biosystems, USA) (94 °C, 3 min; 94 °C, 30 s, 60 °C, 1 min, 72 °C, 1 min, for 40 cycles; 72 °C, 7 min). cDNA was synthesized from 1 µg of total RNA using TaqMan® Reverse Transcription Reagents (Life Technologies, Grand Island, NY, USA) per the manufacturer's instruction. Real-time PCR was performed as described before [41]. All experiments were performed in triplicate and each experiment was repeated at least twice independently.

Western blot analysis

Protein lysates were made from tissues and tumor samples using RIPA lysis buffer (ThermoFisher Inc., USA) containing the complete protease inhibitor cocktail (Roche, USA) and the PhosSTOP phosphatase inhibitor cocktail (Roche, USA). Ten µg of protein lysate was loaded onto sodium dodecyl sulfate-polyacrylamide gel electrophoresis gels and transferred to polyvinylidene difluoride membrane for immunoblotting as described previously [41]. Membranes were probed with antibodies. The following antibodies were purchased from Cell Signaling Technology Inc. (Danvers, MA, USA): AKT, p-AKT (S473), p-RPS6 (S235/236), RPS6, PTEN. Antibody against Menin was purchased from Bethyl Laboratories, Inc. (Montgomery, TX, USA). GAPDH protein was used as a loading control for immunoblots in all the experiments. All the experiments were repeated at least twice independently.

Serum assays

Since MPR mice showed lethargic symptom after 9 weeks, to make sure MPR mice were alive for glucose measurement and blood collection for serum assays, all MPR, control MP littermates, MR, and PR mice were fasted for 3–5 h in the morning before blood collection. MPM and control MP littermates were fasted for 16 h before blood collection. Blood glucose was measured with ONE TOUCH Ultra2 blood glucose meter (Lifescan, Inc., USA). Using the manufacturer's instructions, serum insulin levels were determined with an ultrasensitive mouse insulin ELISA Kit (Crystal Chem Inc., 90080, USA). Serum prolactin, GH, and ACTH levels were measured using commercial kits from Calbiotech (PR063F-100, USA), Millipore (EZRMGH-45K, USA), and Lifespan Biosciences Inc. (LS-F5354, USA), respectively. Serum insulin, prolactin, and GH levels were repeated at least twice independently. Serum ACTH levels was performed once due to limitation of serum.

Rapamycin treatments

The in vivo efficacy of rapamycin treatment on NETs was evaluated in MPR mouse model. One trial was on 4–5-week-old MPR mice and the other was on 7–9-week-old mice. Vehicle and rapamycin (LC Laboratories Inc., Woburn, MA, USA) (15 mg/kg, QWK, I.P.) was injected into mice weekly. Body weight was measured once per week. Pituitary size was measured at autopsy using a ruler. Pituitary and pancreas were examined macroscopically at autopsy. Paraffin-embedded sections were evaluated histologically after H & E and IHC staining.

The in vivo efficacy of rapamycin was similarly evaluated in the MPM mouse model. Treatments were performed on 4-week-old MPM mice. Pancreas was examined at autopsy macroscopically. Paraffin-embedded sections were evaluated histologically after H&E and IHC staining.

Statistical analysis

Graphs were produced using the GraphPad Prism version 6.0b software. The statistical significance of survival curves between two groups was analyzed using log-rank (Mantel-Cox) test, and the statistical significance of pituitary size between two groups was analyzed using unpaired *t* test with Welch's correction by the GraphPad Prism_6.0b software. $p < 0.05$ was considered significant.

Results

Pten and *Men1* function cooperatively to accelerate PitNETs and death

To test our hypothesis that Pten and Menin may function cooperatively to suppress NE tumorigenesis, we investigated whether the MPR compound mice developed NETs earlier than MR or PR mice. We monitored survival of a cohort of MPR mice, alongside MP mice, the single MR or PR deletion mice. MPR mice started dying at 9 weeks and did not live beyond 23 weeks (Fig. 1a), while control MP, MR, and PR mice did not die during the study period, consistent with other studies [25, 42]. Quantitative mRNA and western blot analysis confirmed that Men1 and/or Pten expression was knocked down in the pituitary in representative MPR, MR, and PR mice (Fig. 1b, c). The median survival of MPR mice was 14 weeks. Among the 70 (38F/32M) lethargic MPR mice, 58 mice (83%, 35F/23M) showed symptoms such as blindness, tilted head/body,

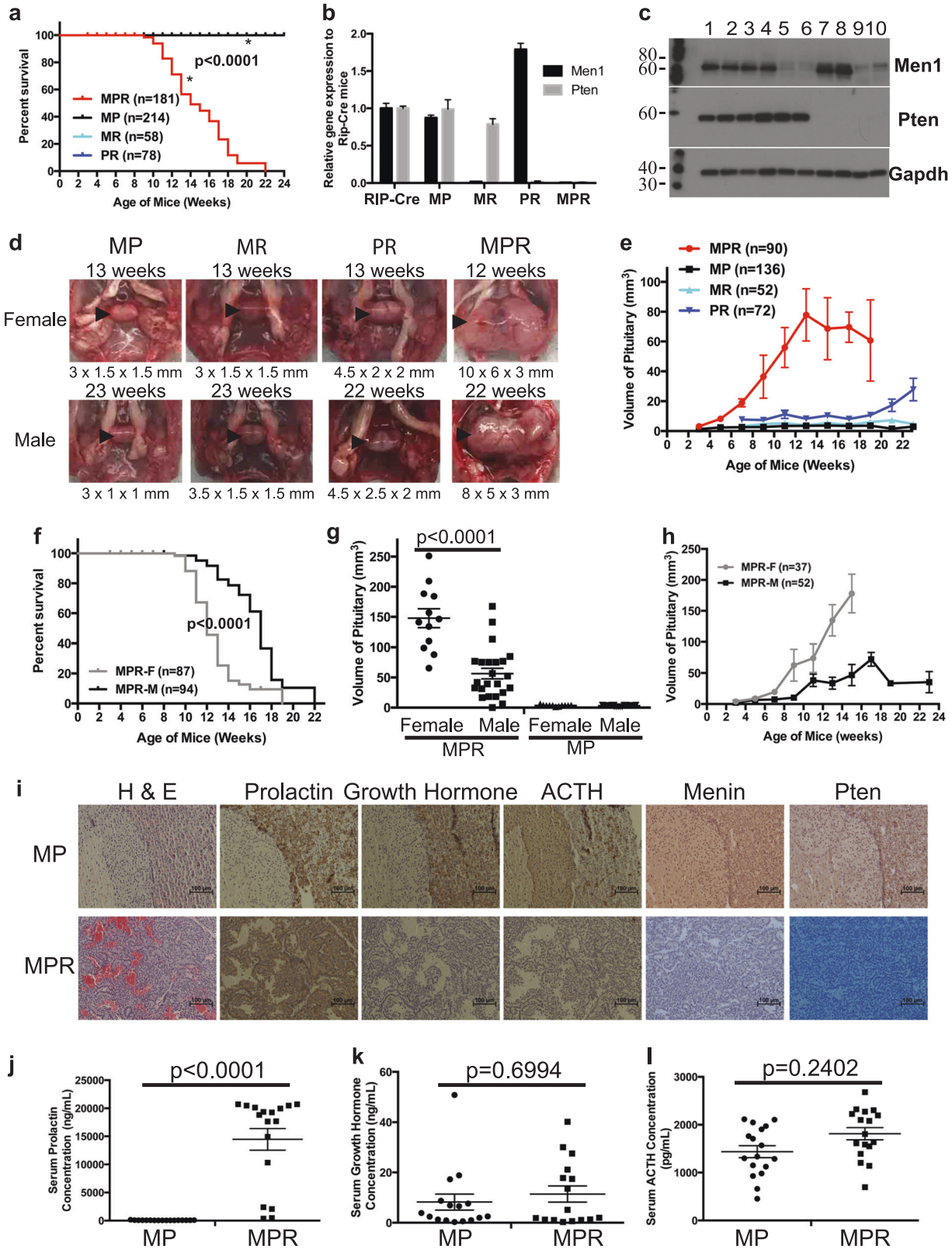

circular gait path, and hind legs paralysis—symptoms consistent with those described in human patients with PitNETs. Autopsy of lethargic mice revealed PitNETs and dramatically enlarged pituitaries. Control MP, MR, and PR mice displayed normal or only slightly enlarged pituitaries (Fig. 1d). Evaluation of the pituitary size over time in a

◀ **Fig. 1** Concomitant loss of *Men1* and *Pten* decreased survival and accelerated pituitary neuroendocrine tumor (PitNET) development in MPR mice. **a** Kaplan–Meier survival curves showed significantly shorter life span ($p < 0.0001$) in MPR mice than in MR, PR, and control MP mice. **b**, **c** Quantitative mRNA and western blots showed that corresponding Men1 or/and Pten gene/protein was deleted in pituitary in the representative mice of various genotypes. **b** Quantitative mRNA analysis. **c** Western blots analysis. Genotypes of each lane: 1 and 2—RIP-Cre; 3 and 4—MP; 5 and 6—MR; 7 and 8—PR; 9 and 10—MPR. The molecular weight markers (in kD) are labeled on the left side of the blots. **d** Gross pathology of pituitary is shown from representative MP, MR, PR, and MPR female mice at 12–13 weeks and male mice at 22–23 weeks. Normal pituitary is cylindrical in shape. The size of pituitary under the image was written as length × width × height (mm). Pituitary is shown with arrowhead inside the mouse skull. **e** Evaluation of the size of pituitaries in 2-week interval starting at 3 weeks (MPR and MP mice) or 7 weeks (MR and PR mice) showed that PitNETs developed dramatically faster and larger in MPR mice. **f** Kaplan–Meier survival curves demonstrated that female MPR mice had significantly shorter life span ($p < 0.0001$) than male MPR mice. **g** Size of pituitary at death in female ($n = 12$) and male ($n = 23$) MPR mice, as well as age-matched female ($n = 11$) and male ($n = 23$) MP mice. **h** Evaluation of the size of pituitaries in female and male MPR mice at scheduled autopsy ($n = 37$ for female mice with $n = 4, 6, 7, 7, 4, 7, 2$ at 3, 5, 7, 9, 11, 13, 15 weeks, respectively; $n = 52$ for male mice with $n = 3, 4, 3, 7, 4, 9, 10, 9, 1, 0, 2$ at 3, 5, 7, 9, 11, 13, 15. 17, 19, 21, 23 weeks respectively). **i** Immunohistochemical staining of prolactin, growth hormones, adrenocorticotropin hormone (ACTH), and Men1 and Pten on pituitary sections in MP and MPR mice. **j–l** Serum hormone levels in MP and MPR mice confirmed that these PitNETs were prolactinomas. **j** Prolactin; **k** Growth hormone; **l** ACTH. MPR $Men1^{flox/flox}$ $Pten^{flox/flox}$ RIP-Cre, MP $Men1^{flox/flox}$ $Pten^{flox/flox}$, MR $Men1^{flox/flox}$ RIP-Cre, PR $Pten^{flox/flox}$ RIP-Cre

cohort of MPR, PR, MR, and MP mice showed that pituitaries grew dramatically faster and larger in MPR mice (Fig. 1e). PR mice showed slightly faster and bigger pituitaries than that in MR and control MP mice during the study period, suggesting that Pten plays a role in suppressing pituitary tumorigenesis. Concomitant loss of *Pten* and *Men1* in mice resulted in earlier onset of PitNETs and death compared to MR and PR mice.

Consistent with the human MEN1 syndrome [43], MPR mice recapitulated a gender bias in tumor development. Assessment of Kaplan–Meier survival (KMS) curves confirmed shortened survival in female vs. male MPR mice (Fig. 1f). Median survival was 12 weeks for females and 17 weeks for males. The PitNETs in female lethargic MPR mice were more than two-fold larger than that in male ones at death, while control female and male MP mice had the same normal size of pituitaries (Fig. 1g). Evaluation of the pituitary size over time in a cohort of MPR mice showed that pituitaries grew faster and larger in female than in male MPR mice (Fig. 1h). This gender bias has also been reported in MR mice [25] and observed in PR mice (Fig. 1d).

To understand the pituitary origin of these tumors, the PitNETs from lethargic MPR mice ($n = 26$, 14F/12M) and the pituitaries from control MP mice were IHC stained for prolactin, GH, and ACTH. Control MP mice showed staining consistent with a normal pituitary—heterogeneous expression of prolactin, GH, and ACTH in the anterior lobe, positive expression of ACTH in the intermediate lobe, and no expression of prolactin, GH, and ACTH in the posterior lobe (Fig. 1i and Supplementary Fig. S2). PitNETs from both female and male MPR mice showed positive staining of prolactin and negative staining of GH and ACTH (Fig. 1i). Evaluation of serum prolactin, GH, and ACTH levels confirmed that these PitNETs were prolactinomas (Fig. 1j–l). Thus these PitNETs arose from the *pars distalis*, mimicking the human MEN1-like syndrome in which prolactinomas are the most common pituitary lesions.

Pten and *Men1* function cooperatively to accelerate PanNETs

We next investigated the effect of the concomitant loss of Pten and Menin in the pancreas, in comparison with the effect of single *Men1* or *Pten* deletion. We evaluated the histopathology of the pancreas for 66 lethargic MPR mice. Fifty-eight mice (88%) developed tumors of variable size and number. From 13 to 22 weeks ($n = 43$), these MPR mice developed multifocal pancreatic tumors that were macroscopically (Fig. 2a) similar to tumors found in MR mice at 35 weeks (11%, $n = 9$) to after 49 weeks (93%, $n = 27$). From 13 to 22 weeks, MR ($n = 34$) and PR ($n = 46$) mice did not show any tumors in the pancreas macroscopically, and evaluation of the histology of pancreas in MR mice ($n = 21$) and PR mice ($n = 25$) did not find any tumors (Fig. 2a and Supplementary Fig. S3A). The protein expression or deletion of Menin and Pten in the islets/tumors of corresponding genotypes was confirmed using IHC staining. IHC staining in MPR pancreatic tumors indicated clonal insulin immunoreactivity, consistent with β-cell neoplasia. Immunoreactivity for the NE markers synaptophysin and chromogranin A indicated that these tumors were PanNETs (Fig. 2b). The Ki 67 index of MPR tumors was between 0.8% and 6.99% (Fig. 2b) and of MR tumors was <2.62% (Supplementary Fig. S3B). By World Health Organization (WHO) classification [1, 3, 4], MPR tumors were G1/G2 PanNETs while MR tumors were G1 PanNETs. The higher Ki 67 index of MPR tumors suggested a higher proliferation rate than that of MR tumors, which may explain early tumor development in MPR mice than that in MR mice. Loss of *Pten* accelerated tumorigenesis in the absence of *Men1* in the pancreas, indicating that *Pten* and *Men1* suppress tumorigenesis of the PanNETs cooperatively in mice. Despite accelerated tumorigenesis, MPR mice maintained WD G1/G2 histology.

To evaluate the temporal appearance and frequency of tumor formation in MPR mice, the histology of their

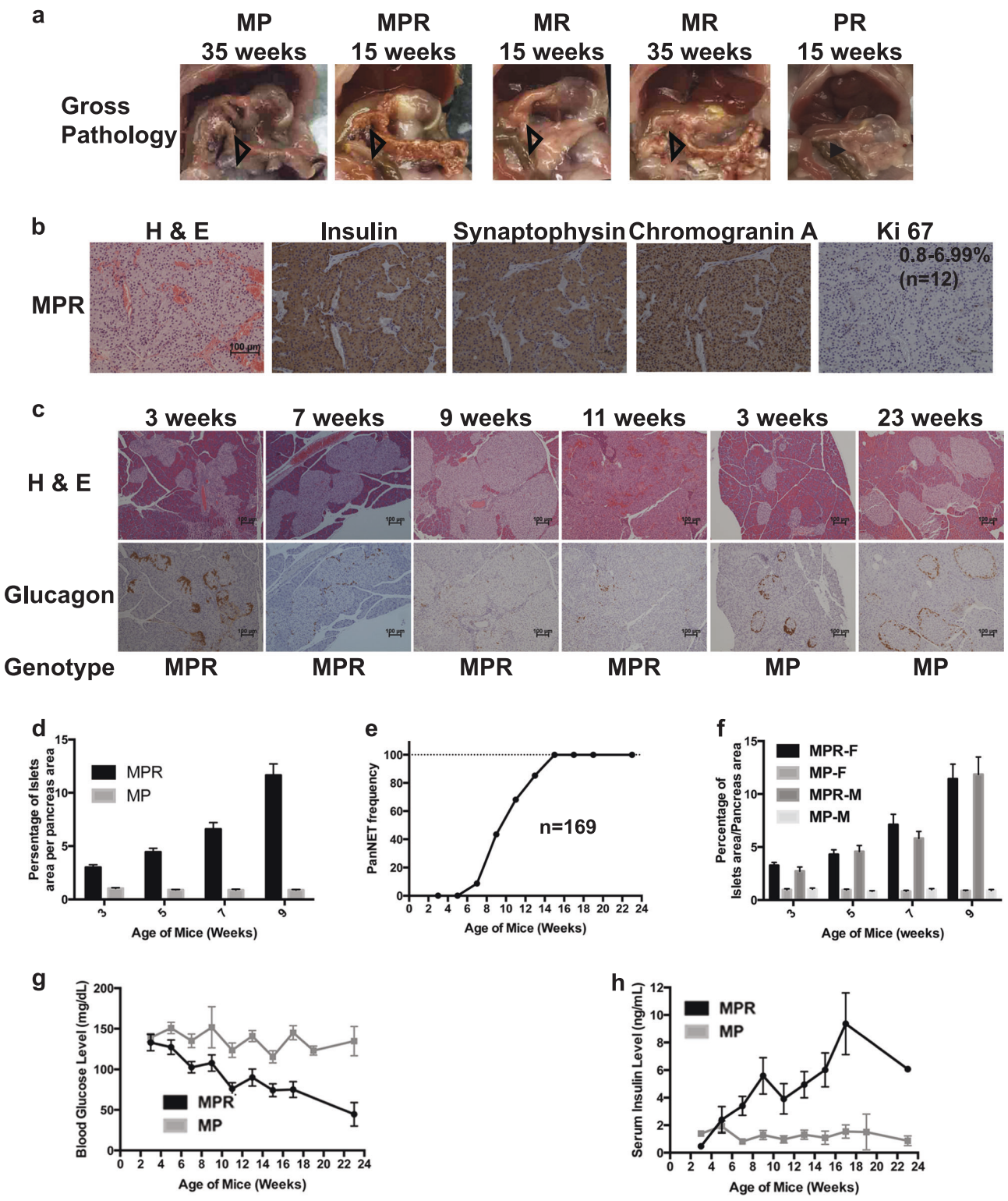

pancreatic islets was evaluated based on H & E and IHC staining of insulin for β-cells and glucagon for α-cells looking at 2-week intervals starting at 3 weeks. Islets from MPR and MP mice showed positive staining for insulin at all time points (Supplementary Fig. S3C). Islets from MP mice were mostly normal with few islets that were mostly round and <0.2 mm in diameter with normal peripheral distribution of α-cells at any age (Fig. 2c). MPR mice showed hyperplastic islets with increasing numbers of small islets and peripheral α-cell distribution starting at 3 weeks.

◀ **Fig. 2** Concomitant loss of *Men1* and *Pten* accelerated pancreatic neuroendocrine tumor (PanNET) development in MPR mice. **a** Gross pathology of pancreas in MP, MPR, MR, and PR mice at 15 or 35 weeks. Pancreas is shown with open triangle inside the mouse abdomen. **b** Hematoxylin and eosin (H & E) and immunohistochemical (IHC) staining of insulin and NET markers on MPR pancreatic tumors. Ki 67 index is shown. **c** H & E and IHC staining of glucagon of pancreas sections from MPR and MP mice of different ages. **d** Quantitative comparison of the ratio of the islets area per pancreas area over time in MP and MPR mice ($n \geq 10$ at each time point). **e** Frequency of PanNETs in MPR mice at the scheduled autopsy ($n = 169$ in total, $n = 12$, 18, 23, 23, 22, 27, 23, 17, 2, 0, 2 at 3, 5, 7, 9, 11, 13, 15, 17, 19, 21 and 23 weeks, respectively). **f** Quantitative comparison of the ratio of the islets area per pancreas area over time in MPR female and male mice ($n \geq 5$ at each time point of each genotype and sex). **g** Blood glucose levels in MPR mice ($n = 133$, $n \geq 11$ of each time point (except $n = 0$ at 19, 21 and $n = 2$ at 23 weeks)) and MP mice ($n = 133$, $n \geq 11$ of each time point (except $n = 4$ at 19, 23 and $n = 0$ at 21 weeks)) and **h** Serum insulin levels in MPR mice ($n = 123$, $n \geq 10$ of each time point (except $n = 0$ at 19, 21 and $n = 1$ at 23 weeks)) and MP mice ($n = 68$, $n \geq 5$ of each time point (except $n = 2$ at 19, $n = 0$ at 21 and $n = 3$ at 23 weeks)) over time. MPR $Men1^{flox/flox}$ $Pten^{flox/flox}$ RIP-Cre, MP $Men1^{flox/flox}$ $Pten^{flox/flox}$, MR $Men1^{flox/flox}$ RIP-Cre, PR $Pten^{flox/flox}$ RIP-Cre

As mice aged, they exhibited increasing size and number of hyperplastic islets, neoplastic islets, and more tumors accompanied by a gradual disappearance of α-cells (Fig. 2c), indicating a multi-step tumor progression. This was further confirmed by quantitatively measuring the ratio of the islets area per pancreas area (Fig. 2d). Histological evaluation in MPR mice showed tumor onset at 7 weeks (8.7%) (Fig. 2e and Table 1), compared to 23 weeks in MR mice [25]. At 15 weeks or later, over 94.7% MPR mice developed PanNETs. Parallel to PanNET formation, MPR mice gradually developed hypoglycemia and increasing serum insulin levels, while MP mice maintained relatively stable blood glucose and serum insulin levels at all ages (Fig. 2g, h). The MPR PanNETs are insulinomas, similar to mouse MR PanNETs.

Rapamycin treatment resulted in delayed growth of PanNETs and PitNETs

To assess signaling alterations in MPR PanNETs and PitNETs, we analyzed the in vivo signaling downstream of Pten and Menin. With Pten loss, Akt, a serine-threonine kinase, is aberrantly phosphorylated and activated in response to PI3K activation. Aberrant activation of mTOR signaling leads to the phosphorylation of downstream effector, ribosomal protein S6 (Rps6). We found increased activation of p-Akt and p-Rps6 in PanNETs and PitNETs in MPR mice (Fig. 3a) as expected with disruption of Pten function.

As a proof of concept and to test the efficacy of our model in preclinical assessments, we set up two trials with the MPR mice using the mTOR inhibitor rapamycin to test for anticancer effects. The first trial tested whether rapamycin treatments could inhibit tumor growth in MPR mice. Treatment started at the onset of tumor development (7–9 weeks). We followed the survival on vehicle-treated mice. When vehicle-treated mice were lethargic, sex-matched, rapamycin-treated littermates ($n = 7$) were sacrificed while other rapamycin-treated mice ($n = 7$) remained in the trial and were sacrificed when six of them were lethargic and one was at 30 weeks to end the treatment. The KMS curve indicated that rapamycin treatments increased the life span of MPR mice ($p < 0.003$; Fig. 3b). Autopsy of these treated mice showed that the pituitaries were significantly smaller in rapamycin-treated mice than in vehicle-treated mice ($p < 0.001$) of the same age (Fig. 3c, d). At death, the pituitaries in rapamycin-treated mice were large and the same size as those of the vehicle-treated mice ($p = 0.50$). The one rapamycin-treated mouse that was alive at 30 weeks had a small PitNET, further supporting that death of MPR mice was due to development of large PitNETs. Similarly, histological examination of the pancreas showed that rapamycin-treated mice exhibited hyperplastic islets while vehicle-treated mice of the same age had PanNETs. Eventually, the rapamycin-treated mice developed PanNETs as well (Fig. 3e). Rapamycin treatment did not show any toxicity based on the measurement of body weight every week (Fig. 3f). Targeting efficacy of rapamycin on these mice was confirmed based on IHC staining of p-Rps6 in these mice (Supplementary Fig. S4E). We also performed a second trial to investigate whether rapamycin treatment could inhibit tumor growth when treatment started before tumor onset (Supplementary section and Supplementary Fig. S4A–D). Collectively, rapamycin treatment delayed the PanNET and PitNET growth but did not inhibit tumor development, and rapamycin treatment increased life span but did not prevent death in MPR mice.

Another GEMM developed only WD PanNETs

The disadvantage of the RIP-Cre construct is that the Cre expression also occurs in the pituitary due to expression of the Insulin 2 gene in hypothalamus [24]. As MEN1 patients could develop both PitNETs and PanNETs in one person in some cases, this MPR model is not necessarily a disadvantage in terms of understanding the molecular mechanism of the human disease. However, it is difficult to use this model as in vivo preclinical model for PanNETs since both PanNETs and PitNETs develop in the same MPR mouse, and PitNETs are the more lethal tumors. A Cre mouse model with Cre gene expression driven by a knock-in mouse Insulin 1 promoter (MIP-Cre) was recently reported to recapitulate the expression pattern of the endogenous mouse Insulin 1 gene with highly specific targeting

Table 1 PanNET frequency in MPR mouse model

Age of mice (weeks)	# of total mice monitored	Tumor frequency of all mice (%)	# of female mice monitored	Tumor frequency of female mice (%)	# of male mice monitored	Tumor frequency of male mice (%)
3	12	0	6	0	6	0
5	18	0	10	0	8	0
7	23	8.7	13	7.7	10	10
9	23	43.5	14	50	9	33.3
11	22	68.2	16	68.8	6	66.7
13	27	85.2	15	80	12	91.7
15	23	95.7	6	100	17	94.1
17	17	100			17	100
19	2	100	1	100	1	100
23	2	100			2	100

PanNET pancreatic neuroendocrine tumor, MPR $Men1^{flox/flox}$ $Pten^{flox/flox}$ RIP-Cre

to the pancreatic β-cells. MIP-Cre expression does not appear in the brain and other tissues [44].

We investigated whether conditional deletion of *Men1* and *Pten* using this promoter would also result in PanNETs. Indeed, MPM mice were healthy with a normal pituitary and developed pancreatic tumors at 24 weeks while MP littermates showed normal pituitary and normal pancreas (Fig. 4a). The tumors from MPM mice stained exclusively positive for insulin and NET markers synaptophysin and chromogranin A, indicating that these were PanNETs (Fig. 4b). The Ki 67 index was between 0.8% and 6.84%. Thus the MPM PanNETs were WD G1/G2 PanNETs consistent with MPR PanNETs.

We then evaluated the temporal appearance and frequency of tumor formation in MPM mice with the same criteria and pancreas-related protocols as with MPR mice. Based on H & E and insulin and glucagon immunoreactivities, MPM mice exhibited the same multi-step tumor progression from hyperplastic islets to one tumor to more tumors as observed in the MPR mice (Supplementary Fig. S5A). Quantitatively measuring the ratio of the islets area per pancreas area confirmed that hyperplastic islets appeared at 3 weeks with progressively increasing the ratio of islets area per pancreas area as PanNETs developed while MP mice displayed consistent ratio of islets area per pancreas area at all ages (Fig. 4c). Histological evaluation of the pancreas of the cohort MPM mice indicated that around 28.6% of MPM mice developed PanNETs at 7 weeks and 100% of mice developed PanNETs at 13 weeks and later (Fig. 4d and Table 2). MPM mice developed hypoglycemia and elevated serum insulin levels as they developed PanNETs (Fig. 4f, g), indicating that these PanNETs were insulinomas, similar to MPR PanNETs. Thus the MPM model showed similar characteristics in the pancreas to MPR mice with no effect on the pituitary.

To understand whether Menin and Pten function cooperatively to suppress PanNETs in MPM mice, pancreas sections from $Men1^{flox/flox}$ MIP-Cre (MM) mice at 18 weeks and $Pten^{flox/flox}$ MIP-Cre (PM) mice at 19 weeks were evaluated histologically. At this age, 100% MPM mice developed PanNETs while MM and PM mice displayed only islet hyperplasia (Supplementary Fig. S5B). MM mice exhibited larger islets and reduced number of α-cells and PM mice exhibited smaller islets with relatively normal distribution of β-cells and α-cells, indicating that MM mice developed more islet abnormalities than PM mice. Quantitative measurements of the ratio of the islets area per pancreas area in the MM and PM mice of 18–19 weeks and in the MP and MPM mice of 11 weeks clearly demonstrated that concomitant loss of *Men1* and *Pten* accelerated PanNET development in MPM mice (Fig. 5a).

To test the efficacy of this MPM model in preclinical assessment, we treated the MPM mice with rapamycin ($n = 13$) and vehicle ($n = 12$) at 4 weeks before the onset of PanNET development. Treatments were ended after 5 weeks in half of the groups of mice and after 8 weeks in the rest of the groups. Histology of the pancreas was evaluated and the ratio of the islets area per pancreas area was quantitatively measured, demonstrating that rapamycin treatments delayed the PanNET growth after 5- or 8-week treatments but did not inhibit PanNET development compared to vehicle-treated littermates (Fig. 5c), as seen in MPR mice. Since MPM mice did not die by 24 weeks, this model provides a better-targeted option for in vivo preclinical therapeutic study for human PanNET patients.

Discussion

Effective models in preclinical testing are essential in improving clinical outcomes. Motivated by the need for WD PanNET models, we sought tumor suppressors that

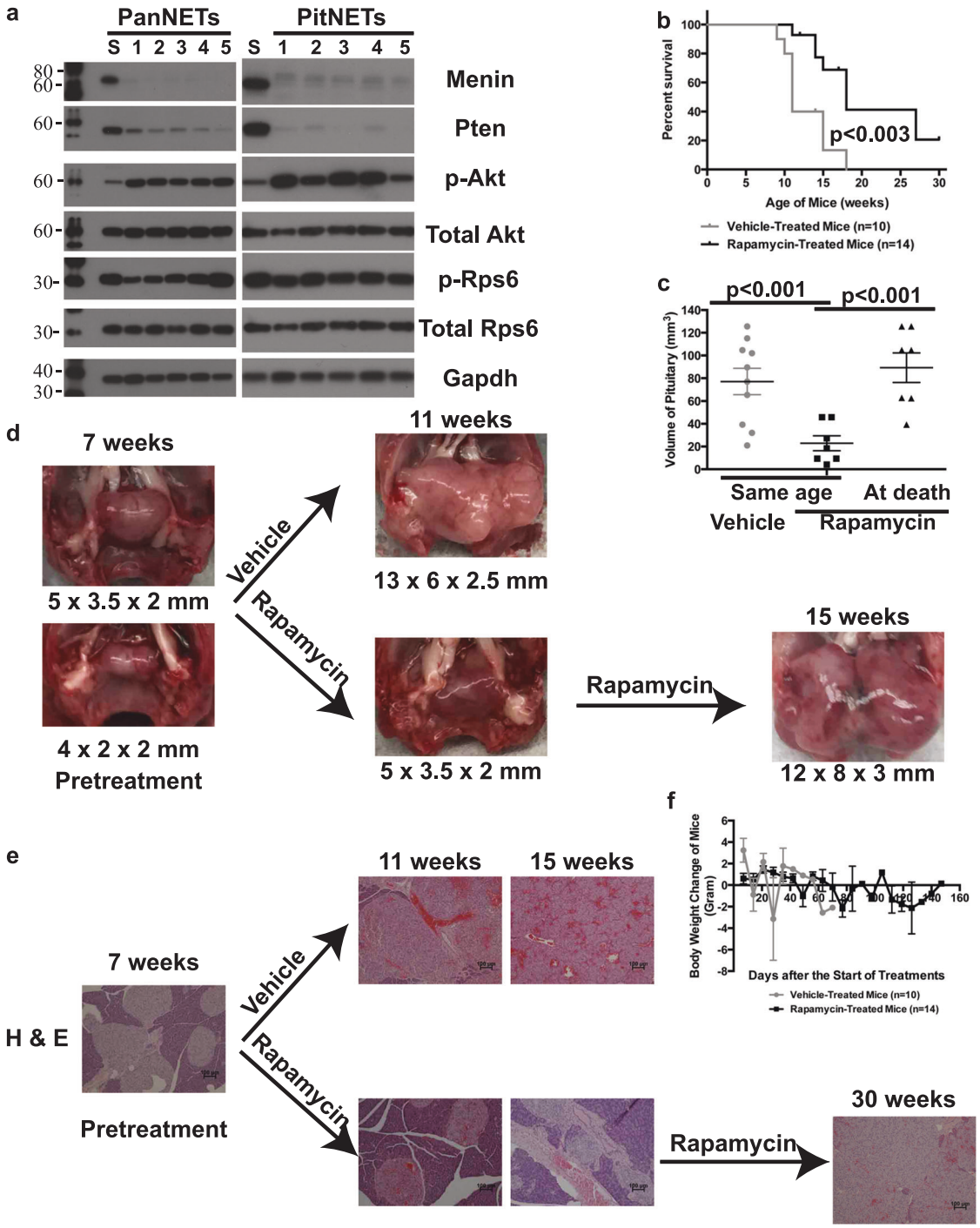

Fig. 3 Rapamycin treatments of MPR mice at the onset of tumor delayed growth of pancreatic neuroendocrine tumors (PanNETs) and pituitary neuroendocrine tumors (PitNETs). **a** Western blot analysis of Menin, Pten, phospho-AKT (p-Akt), total Akt, phospho-Rps6 (p-Rps6), total Rps6, and Gapdh proteins from 5 PanNETs and 5 PitNETs of MPR mice shown in Lanes 1–5. Lane S is the spleen from one of the five MPR mice. The molecular weight markers (in kD) were labeled on the left side of the blots. **b–d** Rapamycin treatment of MPR mice at the onset of tumor delayed growth of PitNETs and death but did not inhibit PitNET development and death in MPR mice. **b** Rapamycin-treated mice ($n = 14$) showed longer life span than vehicle-treated MPR mice ($n = 10$) ($p < 0.003$) in the first trial. **c** Size of PitNETs of vehicle-treated mice ($n = 10$) was significantly larger than rapamycin-treated mice ($n = 7$) of the same age ($p < 0.001$); size of PitNETs of rapamycin-treated mice ($n = 7$) at death/end of treatment was similar to that of vehicle-treated mice at death ($p = 0.5$). **d** Gross pathology of pituitary in vehicle-treated or rapamycin-treated MPR mice in the first trial. **e** Rapamycin treatments delayed the growth of PanNET in MPR mice—H & E of pancreas in vehicle-treated or rapamycin-treated MPR mice in the first trial. **f** Rapamycin was not toxic to mice. Weekly body weight change of rapamycin- and vehicle-treated mice was shown

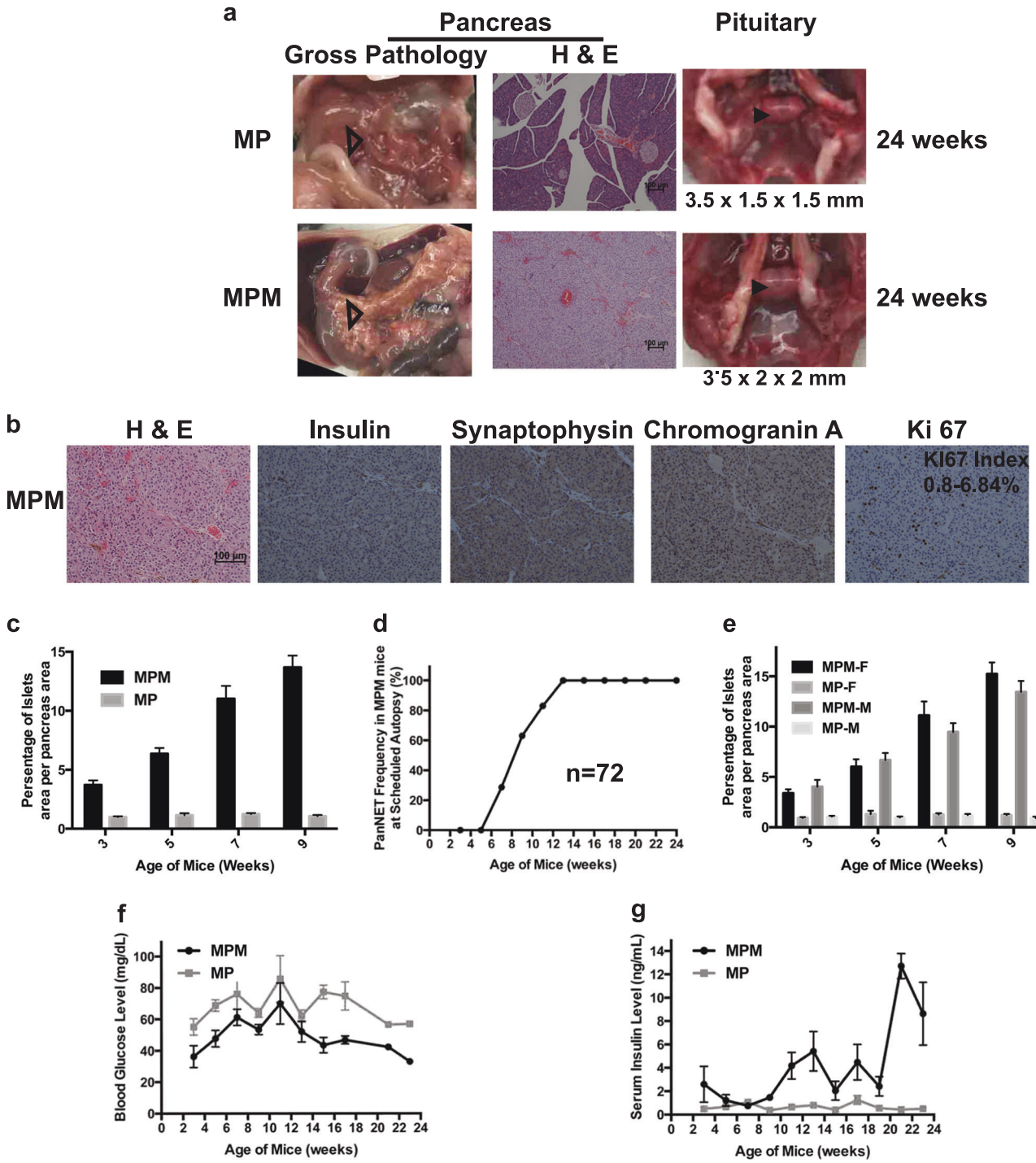

Fig. 4 Another well-differentiated pancreatic neuroendocrine tumor (PanNET) mouse model—MPM. **a** Gross pathology of pancreas and pituitary, and hematoxylin and eosin (H & E) staining of pancreas at 24 weeks in MP and MPM mice. Pancreas is shown with open triangle inside the mouse abdomen and pituitary is shown with arrowhead inside the mouse brain skull. **b** MPM tumors were G1/G2 PanNETs—H & E and immunohistochemical staining of insulin, synaptophysin, chromogranin A, and Ki 67 in MPM mice. Ki 67 index ($n = 16$) is shown. **c** Quantitative measurements of the ratio of the islet area per pancreas area in MP and MPM mice as mice aged ($n \geq 6$ of each time point and each genotype). **d** Tumor frequency in MPM mice ($n = 72$; examined mice at weeks of 3 ($n = 7$), 5 ($n = 7$), 7 ($n = 7$), 9 ($n = 8$), 11 ($n = 6$), 13 ($n = 10$), 15 ($n = 4$), 17 ($n = 12$), 19 ($n = 3$), 21 ($n = 5$), and 23 ($n = 3$). **e** Quantitative measurements of the ratio of the islet area per pancreas area in female and male MP and MPM mice as mice aged ($n \geq 3$ of each time point, each genotype, and sex). **f** Blood glucose levels in MP and MPM mice as mice aged ($n = 65$ for MPM ($n = 7$, 7, 7, 8, 4, 10, 4, 12, 0, 5, 1 at 3, 5, 7, 9, 11, 13, 15, 17, 19, 21 and 23 weeks, respectively) and $n = 64$ for MP ($n = 8$, 8, 7, 7, 4, 12, 7, 7, 0, 3, 1 at 3, 5, 7, 9, 11, 13, 15, 17, 19, 21 and 23 weeks, respectively)) and **g** serum insulin levels in MP and MPM mice as mice aged ($n = 68$ for MPM ($n = 6$, 7, 7, 8, 5, 9, 4, 12, 3, 5, 2 at 3, 5, 7, 9, 11, 13, 15, 17, 19, 21 and 23 weeks, respectively) and $n = 65$ for MP ($n = 8$, 9, 8, 6, 5, 12, 7, 7, 1, 2, 0 at 3, 5, 7, 9, 11, 13, 15, 17, 19, 21 and 23 weeks, respectively)) MPM *Men1*$^{flox/flox}$ *Pten*$^{flox/flox}$ MIP-Cre, MP *Men1*$^{flox/flox}$ *Pten*$^{flox/flox}$, MM *Men1*$^{flox/flox}$ MIP-Cre, PM *Pten*$^{flox/flox}$ MIP-Cre

Table 2 PanNET frequency in MPM mouse model

Age of mice (weeks)	# of total mice	Tumor frequency in all mice (%)	# of female mice	Tumor frequency in female mice (%)	# of male mice	Tumor frequency in male mice (%)
3	7	0	3	0	4	0
5	7	0	3	0	4	0
7	7	28.6	3	33.3	4	25
9	8	63	5	66.7	3	66.7
11	6	83	3	100	3	66.7
13	10	100	5	100	5	100
15	4	100	3	100	1	100
17	12	100	5	100	7	100
19	3	100	3	100		
21	5	100	3	100	2	100
24	3	100	2	100	1	100

PanNET pancreatic neuroendocrine tumor, MPM *Men1*$^{flox/flox}$ *Pten*$^{flox/flox}$ MIP-Cre

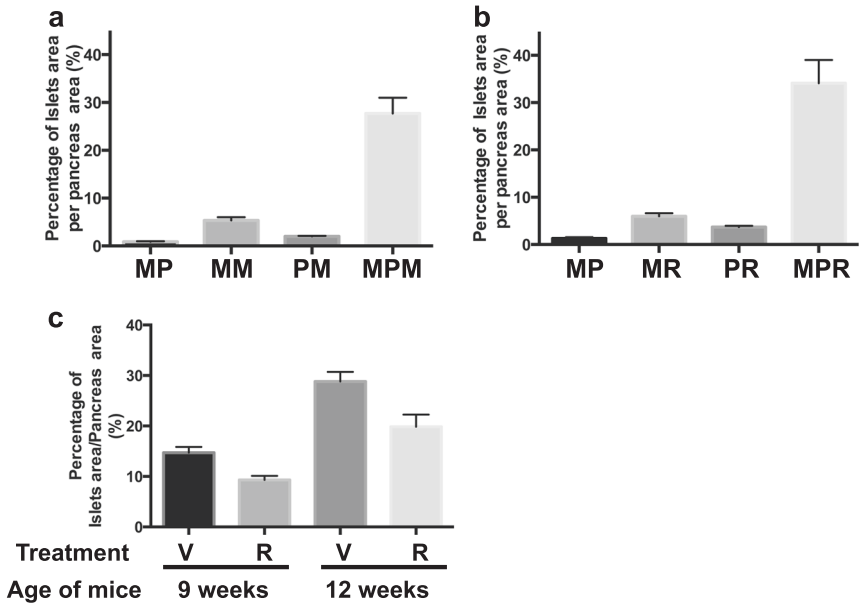

Fig. 5 Concomitant loss of *Men1* and *Pten* accelerated pancreatic neuroendocrine tumor development in MPM mice. **a** Quantitative measurements of the ratio of the islet area per pancreas area in MP ($n = 6$), MPM ($n = 6$) mice of 11 weeks, and MM ($n = 4$) and PM ($n = 6$) mice of 18–19 weeks. **b** Quantitative measurements of the ratio of the islets area per pancreas area in MP ($n = 3$), MR ($n = 3$), PR ($n = 3$), and MPR ($n = 5$) mice of 15 weeks. **c** Quantitative measurements of the ratio of the islets area per pancreas area of treated mice in preclinical rapamycin assessment. Vehicle-treated mice (V) at 9 weeks ($n = 6$), Rapamycin-treated mice (R) at 9 weeks ($n = 5$), Vehicle-treated mice (V) at 12 weeks ($n = 6$), Rapamycin-treated mice (R) at 12 weeks ($n = 8$). MPM *Men1*$^{flox/flox}$ *Pten*$^{flox/flox}$ MIP-Cre, MP *Men1*$^{flox/flox}$ *Pten*$^{flox/flox}$, MM *Men1*$^{flox/flox}$ MIP-Cre, PM *Pten*$^{flox/flox}$ MIP-Cre, MPR *Men1*$^{flox/flox}$ *Pten*$^{flox/flox}$ RIP-Cre, MR *Men1*$^{flox/flox}$ RIP-Cre, PR *Pten*$^{flox/flox}$ RIP-Cre

function cooperatively with Menin to suppress NE tumorigenesis. Using Cre-LoxP system to inactivate *Pten* and *Men1* in β-cells, we generated two mouse models that develop tumors earlier than single deletion of *Men1* or *Pten*: MPR that develops PanNETs and PitNETs in the same mouse, and MPM that develops only PanNETs. Examination of the Ki 67 index of PanNETs indicates that they are WD G1/G2 PanNETs, which are in keeping with the human counterpart PanNETs. The PitNETs developed in MPR mice are prolactinomas, which may be the reason that female mice developed PitNETs faster and larger than male mice. The PanNETs developed in MPR and MPM mice are insulinomas and gender bias was not observed in PanNET development based on the ratio of β-cell mass and tumor

development frequency as mice aged (Fig. 2f and Table 1, Fig. 4e and Table 2).

The rapid development of NETs in MPR and MPM mice suggests that Pten and Menin function cooperatively to suppress NE tumorigenesis. The cooperative function of Menin and Pten has not been previously reported in any cancer. Our data are also the first to directly support the importance of the PI3K/AKT/mTOR pathway in NE tumorigenesis in mice. It has been reported that *Pten* deletion does not lead to tumorigenesis in β-cells in mice [42, 45, 46], even with the co-activation of c-Myc. However, our MPR and MPM models demonstrate that *Pten* deletion plays a role in tumorigenesis in β-cells. This suggests that Pten function cooperatively with Menin but not with c-Myc. Our analysis of the ratio of the islets area per pancreas area between MR and PR and between MM and PM (Fig. 5a, b) suggests that Pten plays a less dominant role than Menin in tumorigenesis of β-cells. In addition, our MPR model suggests that Pten deletion plays a role in tumorigenesis of pituitary, which has not been reported before. PR mice showed faster growth of pituitary than MR (Fig. 1e) and displayed PitNETs eventually (Data not shown), suggesting that Pten may play a more dominant role than Menin in tumorigenesis of pituitary. The functional consequence of Menin inactivation is the loss of H3K4me3 on the promoters of Menin-regulated genes, which leads to downregulation of these genes [47]. In endocrine pancreas, Menin-regulated genes are cyclin-dependent kinase inhibitors *p18* and *p27* [48]. Our evaluation on the expression of p27 and p18 in the MPR and MR tumors suggested low or undetected protein expression in MR and MPR tumors (data not shown). Since it has been reported that Pten controls cell cycle by decreasing cyclin D and increasing p27 expression [49], cooperativity of Menin and Pten in NE tumorigenesis may be through regulation of p27. Further investigation of how Menin-mediated and PI3K/AKT/mTOR signaling pathways function cooperatively is worth pursuing.

The Men1 mouse models closely resemble human MEN1 disease but develop PanNETs at a delayed latency, which is not an ideal preclinical model. The RIP-Tag2 mouse model is well characterized with tumor onset at 10 weeks and has proven effective in drug testing for the treatment of advanced PanNETs [12, 50, 51]. However, RIP-Tag2 mice develop high-grade WD G3 PanNETs and PD PanNECs, which are uncommon in human counterpart PanNETs [15]. In addition, the mouse has a T-antigen not found in human and co-mutations of tumor suppressors Rb and p53 have not been reported in human PanNETs. Our MPR and MPM models have the advantages of both Men1 and RIP-Tag2 mouse models. The MPR and MPM models mimic human MEN1-like disease and develop WD G1/G2 PanNETs. Also, co-mutations of *PTEN* and *MEN1* have been found in 8.8% [32] or 13.3% [21] of human PanNET patients with somatic *MEN1* mutations and in 50% [32] or 80% [21] of human PanNET patients with somatic *PTEN* mutations. Like the RIP-Tag2 model, the MPR and MPM models have an earlier onset of PanNETs. Consistent with expectations for such models, the mice were responsive to the well-established rapamycin treatment. Specifically, MPM model develops only PanNETs, allowing preclinical study of drug candidates for WD PanNETs. Our models will complement the RIP-Tag2 mouse model in PanNET therapeutic research [12, 50].

In summary, we demonstrate for the first time that Menin and Pten function cooperatively in suppression of NE tumorigenesis in pancreas and pituitary and have developed two WD PanNET mouse models, which will permit a more detailed exploration of the pathways in NETs. With their similarity to human NETs, these models could prove valuable in preclinical investigation of much needed new therapies for these indolent but progressive and often fatal tumors.

Acknowledgements We sincerely thank Richard Clausen for breeding the mice and performing genotyping for the project. We would like to thank the Raymond and Beverly Sackler Foundation for their support of our research. We thank Histopathology Services and the Biomedical Imaging shared resources of Rutgers Cancer Institute of New Jersey (P30CA072720) for their support and help.

Financial support This work was supported by the Raymond & Beverly Sackler Foundation.

Compliance with ethical standards

Conflict of interest The authors declare that they have no conflict of interest.

References

1. Bosman FT, Carneiro F, Hruban RH, Theise ND. World Health Organization (WHO) Classification of Tumours of the Digestive System. Lyon: IARC Press; 2010.

2. Tang LH, Untch BR, Reidy DL, O'Reilly E, Dhall D, Jih L, et al. Well-differentiated neuroendocrine tumors with a morphologically apparent high-grade component: a pathway distinct from poorly differentiated neuroendocrine carcinomas. Clin Cancer Res. 2016;22:1011–7.
3. Scoazec JY, Couvelard A, Reseau T. [Classification of pancreatic neuroendocrine tumours: Changes made in the 2017 WHO classification of tumours of endocrine organs and perspectives for the future]. Ann Pathol. 2017;37:444–56.
4. Guilmette JM, Nose V. Neoplasms of the neuroendocrine pancreas: an update in the classification, definition, and molecular genetic advances. Adv Anat Pathol. 2018;26(1):13–30.
5. Yao JC, Shah MH, Ito T, Bohas CL, Wolin EM, Van Cutsem E, et al. Everolimus for advanced pancreatic neuroendocrine tumors. N Engl J Med. 2011;364:514–23.
6. Yao JC, Pavel M, Phan AT, Kulke MH, Hoosen S, St Peter J, et al. Chromogranin A and neuron-specific enolase as prognostic markers in patients with advanced pNET treated with everolimus. J Clin Endocrinol Metab. 2011;96:3741–9.
7. Raymond E, Dahan L, Raoul JL, Bang YJ, Borbath I, Lombard-Bohas C, et al. Sunitinib malate for the treatment of pancreatic neuroendocrine tumors. N Engl J Med. 2011;364:501–13.
8. Strosberg J, Wolin E, Chasen B, Kulke M, Bushnell D, Caplin M, et al. Health-related quality of life in patients with progressive midgut neuroendocrine tumors treated with (177)Lu-dotatate in the phase III NETTER-1 trial. J Clin Oncol. 2018;36:2578–84.
9. Moreno A, Akcakanat A, Munsell MF, Soni A, Yao JC, Meric-Bernstam F. Antitumor activity of rapamycin and octreotide as single agents or in combination in neuroendocrine tumors. Endocr Relat Cancer. 2008;15:257–66.
10. Chiu CW, Nozawa H, Hanahan D. Survival benefit with proapoptotic molecular and pathologic responses from dual targeting of mammalian target of rapamycin and epidermal growth factor receptor in a preclinical model of pancreatic neuroendocrine carcinogenesis. J Clin Oncol. 2010;28:4425–33.
11. Olson P, Chu GC, Perry SR, Nolan-Stevaux O, Hanahan D. Imaging guided trials of the angiogenesis inhibitor sunitinib in mouse models predict efficacy in pancreatic neuroendocrine but not ductal carcinoma. Proc Natl Acad Sci USA. 2011;108:E1275–84.
12. Hanahan D. Heritable formation of pancreatic beta-cell tumours in transgenic mice expressing recombinant insulin/simian virus 40 oncogenes. Nature. 1985;315:115–22.
13. Evers BM, Townsend CM Jr., Upp JR, Allen E, Hurlbut SC, Kim SW, et al. Establishment and characterization of a human carcinoid in nude mice and effect of various agents on tumor growth. Gastroenterology. 1991;101:303–11.
14. Wong C, Vosburgh E, Levine AJ, Cong L, Xu EY. Human neuroendocrine tumor cell lines as a three-dimensional model for the study of human neuroendocrine tumor therapy. J Vis Exp. 2012;66:e4218.
15. Hunter KE, Quick ML, Sadanandam A, Hanahan D, Joyce JA. Identification and characterization of poorly differentiated invasive carcinomas in a mouse model of pancreatic neuroendocrine tumorigenesis. PLoS ONE. 2013;8:e64472.
16. Thakker RV. Multiple endocrine neoplasia type 1 (MEN1). Best Pract Res Clin Endocrinol Metab. 2010;24:355–70.
17. Thakker RV. Multiple endocrine neoplasia type 1 (MEN1) and type 4 (MEN4). Mol Cell Endocrinol. 2014;386:2–15.
18. Thakker RV, Newey PJ, Walls GV, Bilezikian J, Dralle H, Ebeling PR, et al. Clinical practice guidelines for multiple endocrine neoplasia type 1 (MEN1). J Clin Endocrinol Metab. 2012;97:2990–3011.
19. Marini F, Giusti F, Tonelli F, Brandi ML. Management impact: effects on quality of life and prognosis in MEN1. Endocr Relat Cancer. 2017;24:T227–T42.
20. Guru SC, Goldsmith PK, Burns AL, Marx SJ, Spiegel AM, Collins FS, et al. Menin, the product of the MEN1 gene, is a nuclear protein. Proc Natl Acad Sci USA. 1998;95:1630–4.
21. Jiao Y, Shi C, Edil BH, de Wilde RF, Klimstra DS, Maitra A, et al. DAXX/ATRX, MEN1, and mTOR pathway genes are frequently altered in pancreatic neuroendocrine tumors. Science. 2011;331:1199–203.
22. Mohr H, Pellegata NS. Animal models of MEN1. Endocr Relat Cancer. 2017;24:T161–T77.
23. Bertolino P, Tong WM, Herrera PL, Casse H, Zhang CX, Wang ZQ. Pancreatic beta-cell-specific ablation of the multiple endocrine neoplasia type 1 (MEN1) gene causes full penetrance of insulinoma development in mice. Cancer Res. 2003;63:4836–41.
24. Biondi CA, Gartside MG, Waring P, Loffler KA, Stark MS, Magnuson MA, et al. Conditional inactivation of the MEN1 gene leads to pancreatic and pituitary tumorigenesis but does not affect normal development of these tissues. Mol Cell Biol. 2004;24:3125–31.
25. Crabtree JS, Scacheri PC, Ward JM, McNally SR, Swain GP, Montagna C, et al. Of mice and MEN1: insulinomas in a conditional mouse knockout. Mol Cell Biol. 2003;23:6075–85.
26. Zhuang Z, Ezzat SZ, Vortmeyer AO, Weil R, Oldfield EH, Park WS, et al. Mutations of the MEN1 tumor suppressor gene in pituitary tumors. Cancer Res. 1997;57:5446–51.
27. Zhuang Z, Vortmeyer AO, Pack S, Huang S, Pham TA, Wang C, et al. Somatic mutations of the MEN1 tumor suppressor gene in sporadic gastrinomas and insulinomas. Cancer Res. 1997;57:4682–6.
28. Shen HC, He M, Powell A, Adem A, Lorang D, Heller C, et al. Recapitulation of pancreatic neuroendocrine tumors in human multiple endocrine neoplasia type I syndrome via Pdx1-directed inactivation of Men1. Cancer Res. 2009;69:1858–66.
29. Tamborero D, Gonzalez-Perez A, Perez-Llamas C, Deu-Pons J, Kandoth C, Reimand J, et al. Comprehensive identification of mutational cancer driver genes across 12 tumor types. Sci Rep. 2013;3:2650.
30. Missiaglia E, Dalai I, Barbi S, Beghelli S, Falconi M, della Peruta M, et al. Pancreatic endocrine tumors: expression profiling evidences a role for AKT-mTOR pathway. J Clin Oncol. 2010;28:245–55.
31. Kasajima A, Pavel M, Darb-Esfahani S, Noske A, Stenzinger A, Sasano H, et al. mTOR expression and activity patterns in gastroenteropancreatic neuroendocrine tumours. Endocr Relat Cancer. 2011;18:181–92.
32. Scarpa A, Chang DK, Nones K, Corbo V, Patch AM, Bailey P, et al. Whole-genome landscape of pancreatic neuroendocrine tumours. Nature. 2017;543:65–71.
33. Chou WC, Lin PH, Yeh YC, Shyr YM, Fang WL, Wang SE, et al. Genes involved in angiogenesis and mTOR pathways are frequently mutated in Asian patients with pancreatic neuroendocrine tumors. Int J Biol Sci. 2016;12:1523–32.
34. Perren A, Komminoth P, Saremaslani P, Matter C, Feurer S, Lees JA, et al. Mutation and expression analyses reveal differential subcellular compartmentalization of PTEN in endocrine pancreatic tumors compared to normal islet cells. Am J Pathol. 2000;157:1097–103.
35. Chung DC, Brown SB, Graeme-Cook F, Tillotson LG, Warshaw AL, Jensen RT, et al. Localization of putative tumor suppressor loci by genome-wide allelotyping in human pancreatic endocrine tumors. Cancer Res. 1998;58:3706–11.
36. Rigaud G, Missiaglia E, Moore PS, Zamboni G, Falconi M, Talamini G, et al. High resolution allelotype of nonfunctional pancreatic endocrine tumors: identification of two molecular subgroups with clinical implications. Cancer Res. 2001;61:285–92.
37. Lamberti G, Brighi N, Maggio I, Manuzzi L, Peterle C, Ambrosini V, et al. The role of mTOR in neuroendocrine tumors: future cornerstone of a winning strategy? Int J Mol Sci. 2018;19:E747.

38. Liu IH, Ford JM, Kunz PL. DNA-repair defects in pancreatic neuroendocrine tumors and potential clinical applications. Cancer Treat Rev. 2016;44:1–9.
39. Gannon M, Shiota C, Postic C, Wright CV, Magnuson M. Analysis of the Cre-mediated recombination driven by rat insulin promoter in embryonic and adult mouse pancreas. Genesis. 2000;26:139–42.
40. Lesche R, Groszer M, Gao J, Wang Y, Messing A, Sun H, et al. Cre/loxP-mediated inactivation of the murine Pten tumor suppressor gene. Genesis. 2002;32:148–9.
41. Wong C, Laddha SV, Tang L, Vosburgh E, Levine AJ, Normant E, et al. The bromodomain and extra-terminal inhibitor CPI203 enhances the antiproliferative effects of rapamycin on human neuroendocrine tumors. Cell Death Dis. 2014;5:e1450.
42. Nguyen KT, Tajmir P, Lin CH, Liadis N, Zhu XD, Eweida M, et al. Essential role of Pten in body size determination and pancreatic beta-cell homeostasis in vivo. Mol Cell Biol. 2006;26:4511–8.
43. Verges B, Boureille F, Goudet P, Murat A, Beckers A, Sassolas G, et al. Pituitary disease in MEN type 1 (MEN1): data from the France-Belgium MEN1 multicenter study. J Clin Endocrinol Metab. 2002;87:457–65.
44. Thorens B, Tarussio D, Maestro MA, Rovira M, Heikkila E, Ferrer J. Ins1(Cre) knock-in mice for beta cell-specific gene recombination. Diabetologia. 2015;58:558–65.
45. Radziszewska A, Choi D, Nguyen KT, Schroer SA, Tajmir P, Wang L, et al. PTEN deletion and concomitant c-Myc activation do not lead to tumor formation in pancreatic beta cells. J Biol Chem. 2009;284:2917–22.
46. Stiles BL, Kuralwalla-Martinez C, Guo W, Gregorian C, Wang Y, Tian J, et al. Selective deletion of Pten in pancreatic beta cells leads to increased islet mass and resistance to STZ-induced diabetes. Mol Cell Biol. 2006;26:2772–81.
47. Dreijerink KMA, Timmers HTM, Brown M. Twenty years of menin: emerging opportunities for restoration of transcriptional regulation in MEN1. Endocr Relat Cancer. 2017;24: T135–45.
48. Matkar S, Thiel A, Hua X. Menin: a scaffold protein that controls gene expression and cell signaling. Trends Biochem Sci. 2013;38:394–402.
49. Chu IM, Hengst L, Slingerland JM. The Cdk inhibitor p27 in human cancer: prognostic potential and relevance to anticancer therapy. Nat Rev Cancer. 2008;8:253–67.
50. Tuveson D, Hanahan D. Translational medicine: cancer lessons from mice to humans. Nature. 2011;471:316–7.
51. Pietras K, Hanahan D. A multitargeted, metronomic, and maximum-tolerated dose "chemo-switch" regimen is antiangiogenic, producing objective responses and survival benefit in a mouse model of cancer. J Clin Oncol. 2005;23:939–52.